AN ABSTRACT OF THE THESIS OF

Richard Donald Reid for the degree Master of Science

in Department of Chemistry, Division of Analytical Chemistry

presented on November 12, 1974 .

Title: Use of a Tungsten Filament Atomizer in Atomic Absorption Spectrometry.

Redacted for privacy

Abstract approved: _____
Edward H. Piepmeier

A nonflame method for atomic absorption spectroscopy is described. A helical tungsten filament from a commercially available 6-V, 4-A light bulb, heated to incandescence in an argon atmosphere is used to atomize 2-μl aqueous samples for metals analyses. Studies of two hollow cathode lamp tungsten filament orientations, a modulated light source and associated electronics are described. A rough optimization of system variables in order to improve sensitivities and limits of detection is also discussed. A time integrated absorbance recording system is described which gives improved results compared to those obtained with the commonly used peak height measurement techniques.

Atomic absorption sensitivities for Mg, Ag, Cu and Ca are 28, 13.2, 3.7 and 0.8 pg, respectively, and corresponding detection limits are 5.2, 16.0, 3.4 and 0.95 pg.

Use of a Tungsten Filament Atomizer In Atomic Absorption Spectrometry

by

Richard Donald Reid

A THESIS

submitted to

Oregon State University

in partial fulfillment of
the requirements for the
degree of

Master of Science

Completed November 12, 1974

Commencement June 1975

APPROVED:

Redacted for privacy

Associate Professor of Chemistry in charge of major

Redacted for privacy

Chairman of Department of Chemistry

Redacted for privacy

Dean of Graduate School

Date thesis is presented November 12, 1974

Typed by Eileen Reid for Richard Donald Reid

TABLE OF CONTENTS

LIST OF TABLES

LIST OF ILLUSTRATIONS

LIST OF ILLUSTRATIONS (Continued)

USE OF A TUNGSTEN FILAMENT ATOMIZER IN ATOMIC ABSORPTION SPECTROMETRY

I. INTRODUCTION

A great deal of current research in the field of analytical chemistry has been aimed at providing more sensitive and selective analytical methods for the determination of trace metals. Atomic absorption spectroscopy (AAS) has proven to be a very useful tool for such determinations. In the last few years, a great amount of research in AAS has been directed toward increasing sensitivity and detection limits through improvement of atomization efficiency or development of new atomization techniques. During the mid-1960's it was realized that the high temperature flame (2000-3500^{o}C) had been studied and improved to the point where no significant improvements in sensitivity (g/1% absorption), in detection limits (the minimum amount which can be observed with a given degree of confidence) and in elimination of matrix effects could be made (1). Thus, it seemed that the improvement of these variables could only be obtained by turning to alternate, more efficient methods of atomization.

It seems to be a well established fact (2) that the atomization process for AAS is purely thermal in nature. Thus, one needed only to find a method of heating up molecules to a sufficiently high temperature (2000-3500^{o}C) to shift the equilibrium between atoms and molecules toward the side of the former. Flames supply the necessary thermal energy but with many disadvantages.

For instance, the violent chemical reaction in a flame creates a chemically impure medium for the reactive analyte atom. The analyte can combine with other elements and compounds to form oxides, carbides and ionic salts which often are refractory in nature. The overall effect is that only a small fraction of the analyte is in atomic form because of reactions such as

$$M + CO \rightleftharpoons MO + C.$$

Since the absorbance is proportional to the atomic population, compound formation reduces the absorbance for a given amount of analyte.

Another disadvantage can be found in the size and inhomogeneity of the flame. The analyte species becomes spread out as it is aspirated into the flame. Thus, the volume element of the flame which is viewed by the monochromator is only a fraction of the total. The positioning of this volume element with respect to the flame is also very critical. The optimum viewing area for refractive elements is usually the hottest part of the flame which is located at the upper tip of the inner cone.

The sample atomization can be greatly affected by the characteristics of the solvent such as viscosity, volatility and salt concentration. It is important that the solvent be quickly vaporized so that the atomization can occur rapidly. It is also significant that the solvent may greatly cool the flame throughout this process. Non-flame techniques essentially eliminate the solvent problem by evaporating the solvent, if it is present, prior to atomization.

Flames themselves exhibit absorption, emission and scattering effects. For most types of flames, absorption and scattering occur significantly below 200 nm. Band emission can be found in regions such as 300-350 nm for OH bands, 250-400 nm for O_2 and 314-432 nm for CH bands. The net result is a very noisy signal in regions where background signals are significant due to flame flicker and shot noise.

The first nonflame instrumentation for AAS was described by L'vov in 1961 (3) and consisted of a modified version of a graphite furnace first used by King (4). This graphite cylinder was 30-50 mm long and had an inner diameter of 2.5-3.0 mm. The radiation beam was focussed down the center of the horizontal furnace. The sample was introduced into the cylinder by means of a vertical carbon electrode with the solution sample in a small cup at the top. The electrode tip was moved up into a fitted hole in the center of the cylinder.

Initially atomization was accomplished by a short d.c. arc pulse between the cylinder and the sample electrode. This proved inefficient because heating was uneven, especially at the ends of the cylinder. In the next ten years L'vov made extensive studies and improvements. In 1967 L'vov proposed an improved vaporization system in which the electrode and cylinder were electrically heated by an a.c. current (5) supplied from a four kW transformer. This allowed better temperature programming, and better results were obtained. L'vov heated the electrode and cylinder separately since the electrode provided for atomization, while the cylinder maintained the atomic population.

It was also discovered that sample atoms diffused into the surface of the graphite furnace leading to contamination or "ghosting" effects during later sample runs. To solve this problem, the inside walls were lined with tantalum or tungsten foil. Later the cylinders were lined with a thin layer of pyrographite (5). The later modification not only stopped vapor diffusion, but also provided more uniform heating. This procedure became almost universal in later nonflame methods which used graphite or carbon. In order to cut down vapor diffusion through the ends of the cylinder and atomospheric interferences, the furnace was enclosed in a chamber equipped with quartz windows. Prior to atomization the chamber was purged with a gas such as argon or nitrogen.

The apparatus was comparatively complex, expensive and required skilled technicians to provide the temperature programming. The relative precision which L'vov reported was only about five percent, but detection limits were excellent (1), i.e., in the nanogram to picogram region for most metals. Tables I and II contain an overall summary of the general properties of L'vov's instrumentation, sensitivities and detection limits germane to this work as well as those of the other instruments yet to be described.

Due to the poor reproducibility of L'vov's furnace, it was virtually ignored for a number of years until 1969 when West, et.al. (6,7) and Robinson, et.al. (8, and in 9) reported nonflame atomizers to the Atomic Absorption Conference in Sheffield, England.

TABLE I. SUMMARY OF GENERAL PROPERTIES FOR OTHER NONFLAME INSTRUMENTS.

Author	Sample size	Gas flow	Duration of peak	Detection system	Recording device
L'vov (3,5)	1-10 µl	purged & sealed	0.5 sec.	Mechanically chopped hollow cathode lamp emission, narrow band RC filter amplifier	Recording potentiometer traverse time: 2 sec./full scale
West (6,7)	5 µl	1-4 l/min.	0.05 sec.	Mechanically chopped hollow cathode lamp emission with an a.c. amplifier	Viscorder Oscilloscope
Robinson (8)	continuous flow	1-5 l/min.	indefinite	Double beam (hollow cathode and continuous sources) with a difference amplifier	Servo recorder
Massmann (10)	1-10 µl	1-5 l/min.	10-20 sec.	Unknown	Unknown
Varian (2) (carbon cup)	5-10 µl	1-10 l/min.	1-3 sec.	Simple current-to-voltage converter with a 0.2 second time constant	Oscilloscope
Perkin-Elmer HGA-70 (11)	1-100 µl	1.5 l/min.	0.10 sec.	Perkin-Elmer spectrometer	Strip chart recorder

TABLE I. (Continued)

Author	Sample size	Gas flow	Duration of peak	Detection system	Recording device
Woodriff (12)	50 µl	40 ml/min.	1-3 min.	Tuned a.c. amplifier with a mechanically chopped hollow cathode lamp emission	Heath recorder
Donega (13)	100 µl	Vacuum	0.05 sec.	Mechanically chopped hollow cathode lamp emission with a lock-in amplifier	Recording oscilloscope
Winefordner (14) (AF)	1 µl	10 l/min.	0.05 sec.	Double beam-difference amplifier	Recording oscilloscope
Goode, Montaser and Crouch (15) (AF)	0-5 µl	2-3 l/min.	0.05 sec.	Simple current-to-voltage amplifier, computer controlled process	PDP-8 performing digital integration
Williams and Piepmeier (16)	3 µl	10 l/min.	0.1-0.3 sec.	Double beam with a difference amplifier	Recording oscilloscope

TABLE II. SENSITIVITIES AND DETECTION LIMITS IN PICOGRAMS.

Author	Ag		Ca		Cu		Mg	
	sens.	d.l.	sens.	d.l.	sens.	d.l.	sens.	d.l.
L'vov (3)	0.1	0.5	0.4	25	0.6	6.3	0.04	3
West (6,7)	600	2000	--	--	33	50	--	--
Massmann (10)	0.8	--	--	--	10.0	--	0.5	--
Perkin-Elmer HGA-70 (2)	--	--	3.1	4.0	45	40	--	--
Varian (2)	1.2	0.2	0.65	0.3	20	7.0	0.43	0.06
Woodriff (12)	8	12	100	530	90	320	80	25
Winefordner (14)	2	--	200	--	--	--	4000	--
Williams and Piepmeier (16)	--	--	3	20	20	10	70	10
Horizontal filament*								
(peak absorbance)	13.2	16.0	0.8	.95	3.7	3.4	28	5.2
(integration)	.0053 mv/pg	8.5	--	--	.002 mv/pg	2.0 pg	--	--

Temperatures: drying T = 100°C; prefire T = 1300° ± 30°C; fire T = 2000° ± 15°C.
Sensitivity is defined as that quantity of the analyte which yields a signal of 1% absorption.

* Resonance lines used in this study for Ag, Ca, Cu and Mg are 328.1 nm, 422.7 nm, 324.8 nm and 285.2 nm, respectively.

West, et.al. (6) reported a new device which he called a carbon filament atomizer. A carbon rod 2 mm in diameter and 20 mm long was supported by two water cooled stainless steel electrodes. A five-second current pulse of 100 A at 5 V heated the filament to 2000-2500°C. Liquid samples were placed on the filament. Early models of the filament were housed in a chamber fitted with quartz windows and purged with argon, similar to L'vov's instrument. In later models the protective chamber was eliminated and a sheath of argon flowing up from underneath the filament was used to protect the carbon and the analyte atoms from the atomosphere and to improve precision. Sensitivities (g/1% absorption) and detection limits were comparable to those of L'vov. However, interferences from volatile matrix elements seemed to be greater, and only the most easily atomized elements could be measured. These difficulties arose because the atomic vapor had to be viewed at some distance from the hot filament to minimize the blackbody emission signal and hence, the shot noise in the emission from the filament. The cooler temperature away from the carbon resulted in atom recombination or compound formation. The temperature difference even one millimeter away from the graphite surface is significant.

The use of this technique for routine analysis was virtually impossible because of the need for complicated heating and cooling processes for reproducible quantitative results. However, interferences due to refractory oxides appeared to be less important than in flames, which is a distinct advantage of this technique.

Cantle and West (7) replaced the graphite filament with a cylindrical tungsten filament 60 mm long and 2.2 mm in diameter that had been ground to produce a recess 1 mm deep by 2 mm wide at its center. One-microliter samples could be placed in this recess, and atomization proceeded as before.

Sensitivities were improved using the tungsten filament, and matrix effects were reduced considerably. This was partially due to the fact that the sample solutions did not penetrate the surface as they did on the carbon filament. Filament lifetime also proved to be an advantage for tungsten over the carbon filament. The latter needed to be replaced every 100-200 runs while the former lasted indefinitely.

The nonflame atomizer of Robinson, et.al. (8,9) was designed for the direct determination of metal oxides in the air. Air was forced over chunks of carbon heated to about 1400^{o}C by an r.f. coil. The oxygen in the air combined with the carbon to form carbon monoxide which then reduced the oxides to metallic form. The resulting atomic vapor was then passed through an absorption chamber 410 mm long and 25 mm in diameter and closed at the ends by quartz windows. The atomic vapor concentration remained constant since the vapor was continually being flushed out exhaust ports by a replenishing supply.

Very effective atomization could be obtained and sensitivities for the more volatile metals were in the range of 0.01 $\mu g/m^3$ or $0.2\text{-}2 \times 10^{-11}$ g absolute sensitivity (g/1% absorption). Some corrections for molecular absorption were made by using a continuum

light source to measure molecular absorbance at the wavelength of the resonance lines.

Massmann built a simplified version of the King-L'vov furnace (10) that was 51 mm long and 8.6 mm in diameter. Its further simplified structure (11) has been developed into a commercial instrument marketed by Perkin-Elmer called the HGA-70 and later the HGA-2000. The hollow cathode beam was focussed down the center.

In the middle of the cylinder there was a hole for sample injection. The furnace was then purged with argon or nitrogen. The gas entered by means of five small holes located intermittently in the cylinder and left through the open ends. The entire structure was water cooled by means of a steel jacket. An automatic current program in three steps dried, ashed and finally atomized the sample. Sensitivities (g/1% absorption) in the tens of picograms were obtained for many elements with precisions of three to eight percent, in the optimum range. This instrument could handle both liquid and solid samples.

Varian Techtron laboratories modified the device of West, et.al. (2) for commercial purposes. Three variations were studied:

1. To hold the sample, either a small hole was drilled through the rod (the mini-Massmann furnace) or an indentation was made on the top of the rod.

2. A chimney was placed beneath the rod to permit the introduction of laminar flow of the sheath gas.

3. Hydrogen was added to the argon which ignited when in contact with the hot filament; this resulted in improved atomization because of reduction in the interelement interferences and non-atomic absorption.

Varian's mini-Massmann device (2) combined characteristics of the carbon filament of West with the Massmann furnace. A rod 5 mm in diameter was used with a transverse hole 1.5 mm in diameter giving the appearance of a small furnace. This device could accommodate a sample size of only 2 µl or less, which tended to decrease precision because of the difficulty of delivering such small samples. Gouging of the internal part of the hole by the metal tip of the microsyringe led to even poorer precision.

The mini-Massmann was then improved (2) by replacing the center of the rod which contained the hole with a large horizontal "tube" furnace 9 mm long and 3 mm in diameter which was perpendicular to the rod. Thus, larger sample sizes (5-10 µl) could be used, plastic tipped syringes replaced metal tips and absolute detection limits were reduced by roughly an order of magnitude. A variation of this involved a vertical cup with a hole drilled through the side for the hollow cathode beam. The latter two types are currently being marketed by Varian Techtron.

Woodriff and Ramelow (12) adapted L'vov's cylinder into a larger furnace 26 mm long and 6 mm in diameter. The sample electrode was eliminated and sample was transported into the cylinder as a fog. A solution nebulizer created the fog from 50 µl of solution and the mist was pumped into the furnace. Atomization occurred in the electrically heated cylinder, whereas L'vov's furnace was only heated to maintain the atom concentration produced by the sample electrode. The major

disadvantage of this instrument was that aqueous solutions could not be nebulized efficiently, and methanol became the principle solvent.

Donega and Burgess (13) have described an instrument which used a graphite, tantalum or tungsten boat enclosed in a selected atmosphere chamber. The sample boats were cut from a 5-mil graphite, 1-mil high purity tungsten or tantalum foils and were about 50 mm long and 6 mm wide. The tantalum and tungsten boats were shaped to provide a small indentation which could hold about 100 µl of solution. In the case of graphite, transverse slits were cut and could hold about 50 µl of solution. Power for heating was supplied by a step-down transformer-variac source which could deliver 30-50 A at 12 V. This current is sufficient to heat the boats to about 2200°C in less than 0.1 second.

The boat was enclosed in a sample chamber with quartz windows for a hollow cathode beam. One end was removable for sample application purposes. The sample was dried and the chamber evacuated to a pressure of 5×10^{-5} torr. Argon was then allowed in to bring the pressure to 1-300 torr, and then the sample was vaporized. The presence of the foreign gas at reduced pressures reduced the diffusion rate of the absorbing species from the light path and resulted in a stronger absorption signal. Sensitivities were comparable to other nonflame instruments, but lower power requirements proved to be a distinct advantage over most furnace systems.

To date, little work has been done on the feasibility of using heated platinum or tungsten wires as a means of atomization. Winefordner, et.al. (14) has studied the use of platinum in atomic

fluorescence spectroscopy. Platinum was chosen because of its inertness, high melting point and low power requirements to produce maximum incandescence (3.3 W maximum compared to 25 W for tungsten before melting occurred). Thirty-one gauge wires that were 2 cm long were twisted into a loop with a diameter of 1/32 inch. The ends of the wire were supported inside a sheath of argon by two brass electrodes 1.0 inch long and 0.04 inch in diameter. These rods were held in electrical terminal post clips attached to Bakelite mounts and then connected to the output of an a.c. stepdown transformer with a variac on the input. The ohmic resistance of the leads and brass rods was negligible compared to that of the loop. The loop could be heated reproducibly to high temperatures without oxidation and burn-out.

Samples were placed on the filament by dipping the loop in the solution. The solvent was then driven off and the sample vaporized. As in carbon filament techniques, the atomized metals are carried up into the beam of the excitation source by the inert gas flow. Peak absorption and integrated peak signals were recorded and found to decrease with increased flow rate. Atomic fluorescence (AF) results were comparable to absorption and fluorescence data in flames. Detection limits compared favorably with AAS and AF using graphite furnaces. This technique has proven useful for elements such as Ag, Bi, Cd, Cu, Hg, Mg, Pb and Zn.

Goode, Montaser and Crouch designed an automated system (15) using Winefordner's AF loop atomizer. They also studied the

optimization of interdependent variables such as applied power and sheath gas flow and the effect of these on atomizer temperature. The objective was the highest possible signal-to-noise ratio. Complete automation yielded high reproducibility which separated sampling effects from other causes of imprecision.

Computer controlled integration was found to yield the best linearity and precision for calibration curves. The optimized results had a detection limit for cadmium 50 times better than Winefordner's results. Reproducibility was four to seven percent.

The work that preceded the technique to be described here was initiated by Williams and Piepmeier (16). A rigid spiral-wound tungsten filament from a commercially available precision light bulb (General Electric No. 1763) was used to atomize 1-5 µl samples. The filament, normally from a 6-V, 4-A light bulb, was powered by a programmable precision power supply.

The lamp was prepared for use by carefully breaking the glass and cleaning off the protruding edges. The base flange of the lamp was mounted on a brass plate which served also as one electrode. The other electrical connection was made by soldering a wire onto the base connector of the lamp base. This complete assembly was mounted in a burner housing with the central axis of the helical filament in a vertical position. The helix and its supporting rods were then enclosed in a vertical quartz tube one-half inch in diameter. To shield the tungsten from the atmosphere, argon was passed at constant

flow rate through the tube creating laminar flow around and through the helical filament. A hollow cathode beam was focussed on a point directly above the filament helix by means of a quartz lens. After the beam had passed over the filament, a 1-mm aperture was placed so that only a small volume directly above the filament was viewed. The resulting beam was split, and these beams were sent through two monochromators and finally through two photomultiplier tubes.

Sample solutions of 1-3 μl were placed on the filament by a micro-syringe with the droplets being held in the center of the helix by surface tension. The filament was heated at 0.45 V for 20 seconds until the water of the sample had been completely evaporated. Then the filament was switched to 4.0 V to atomize the sample. Free atoms flowed up into the path of the hollow cathode beam and absorption occurred. The signal due to tungsten blackbody emission was compensated for by the second monochromator which looked at a wavelength close to the resonance line of the hollow cathode. The difference in the signals from the two monochromators was monitored on a storage oscilloscope. Still some difficulty with blackbody emission occurred in the visible region.

Sensitivities (g/1% absorption) and limits of detection (concentration at which the signal-to-noise ratio equals unity) were about an order of magnitude poorer than for other nonflame instruments. This could be partially due to cooler atomic vapor temperatures compared to other nonflame instruments. Cooler atom temperatures resulted in increased matrix effects.

Absorbance calibration curves were linear up to 50 percent absorption. Reproducibility for peaks of intermediate size (50-70% T) was about five percent.

In all of the nonflame methods described, several distinct advantages seem evident. First of all, these systems provide high absolute AA sensitivity and low limits of detection, i.e., in the picogram range. Samples in many different forms, liquid or solid, can be run without regard to viscosity or solvent volatility, which would make aspiration into a flame prohibitive. Sample size can run from 1-100 µl which for sample-limited situations such as in biomedical analysis would be particularly useful. However, along with the small sample size requirements comes a critical problem. Microliter aliquots are subject to a high sampling error (approximately five percent).

In order to fully exploit this type of instrumentation, new developments in the area of simplified operation for routine work, smaller sampling errors and more efficient peak or area measuring devices must be made. Lower cost is also an important objective.

The research reported in this work was done to delve into these problems and improve the system designed by Williams and Piepmeier (16). Specifically, attempts were made to improve sensitivities and limits of detection by means of changing the filament positioning and improving the absorption peak area recording system.

II. INSTRUMENTATION

In this section the atomization, optical and electronic instrumentation are described. The construction of the different parts of the instrumental system are illustrated in Figures 1-5, and the specific commercial components used are listed in Table III.

A. The Filament and Mounting

As in the work of Williams and Piepmeier (16), sample atomization is achieved by means of the heated rigid spiral-wound tungsten filament found in a commercial 6-V, 24-W light bulb (General Electric No. 1763). The tungsten wire used in this spiral filament is 0.19 mm in diameter; the helix has an outer diameter of 1.25 mm and contains seven turns of wire for an overall length of 1.13 mm.

To prepare the lamp for use as an atomizer, the glass bulb is broken off carefully and completely to expose the filament and supports. This work studied two positions of this filament. First, the original mounting assembly described by Williams and Piepmeier (16) was used in which the central axis of the filament was vertical and perpendicular to the hollow cathode-monochromator axis. Later, the filament was turned so that its central axis was in line with the hollow cathode-monochromator axis, and the filament was mounted on an x-y optical bench for easy adjustment and alignment. Figure 1 shows the optical bench assembly which includes the filament, supports and protective shielding.

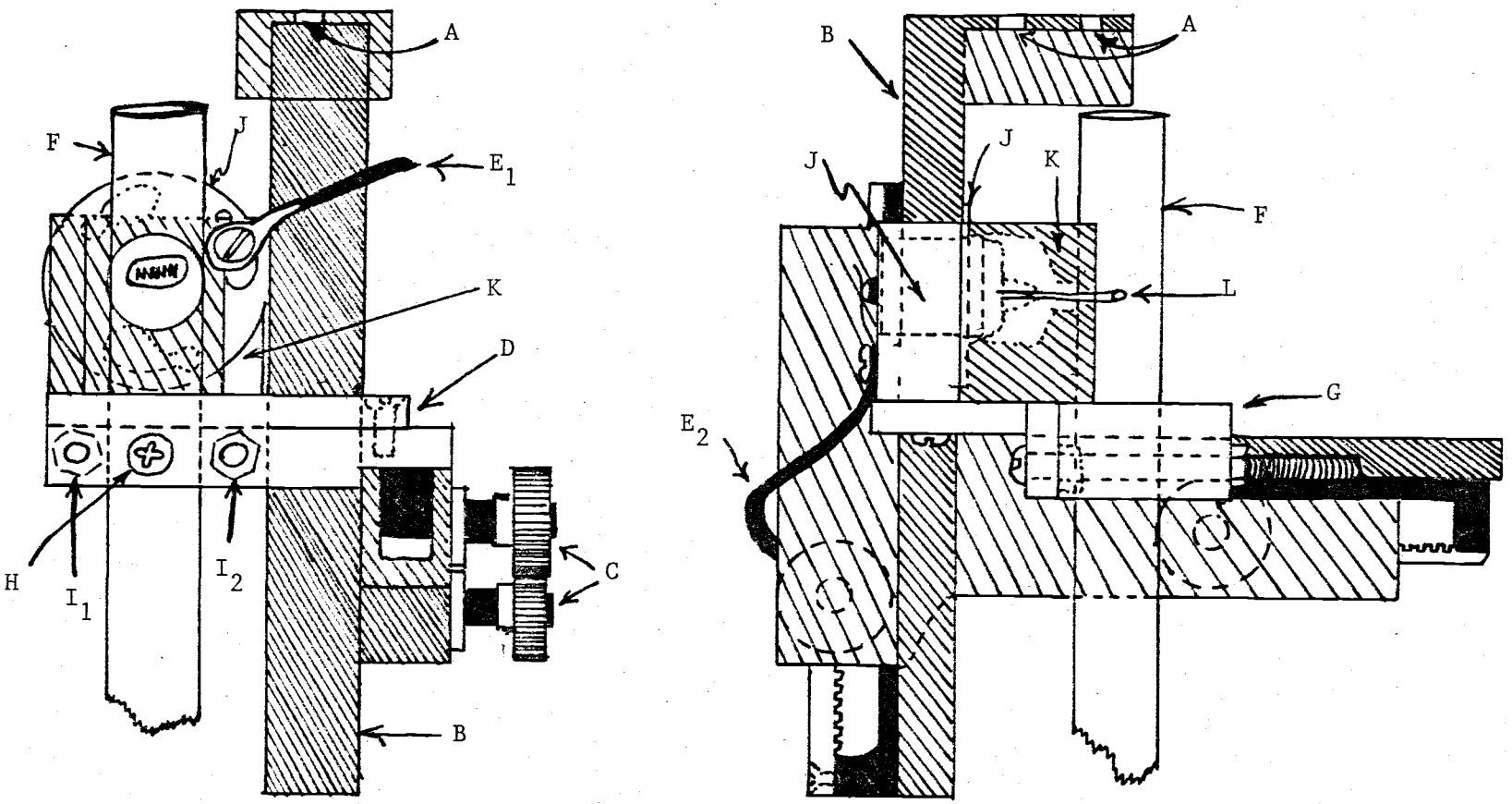

Figure 1. 1:1 drawing of filament assembly mounting.

A. Mounting holes
B. X-Y optical bench (shaded area)
C. X-Y adjustment knobs
D. Filament assembly mounting
E. Voltage wires
F. Quartz glass tube
G. Quartz tube mounting bracket
H. Quartz lube set screw
I. Bracket mounting nuts and bolts
J. Light bulb flange
K. Filament protector
L. Tungsten filament helix

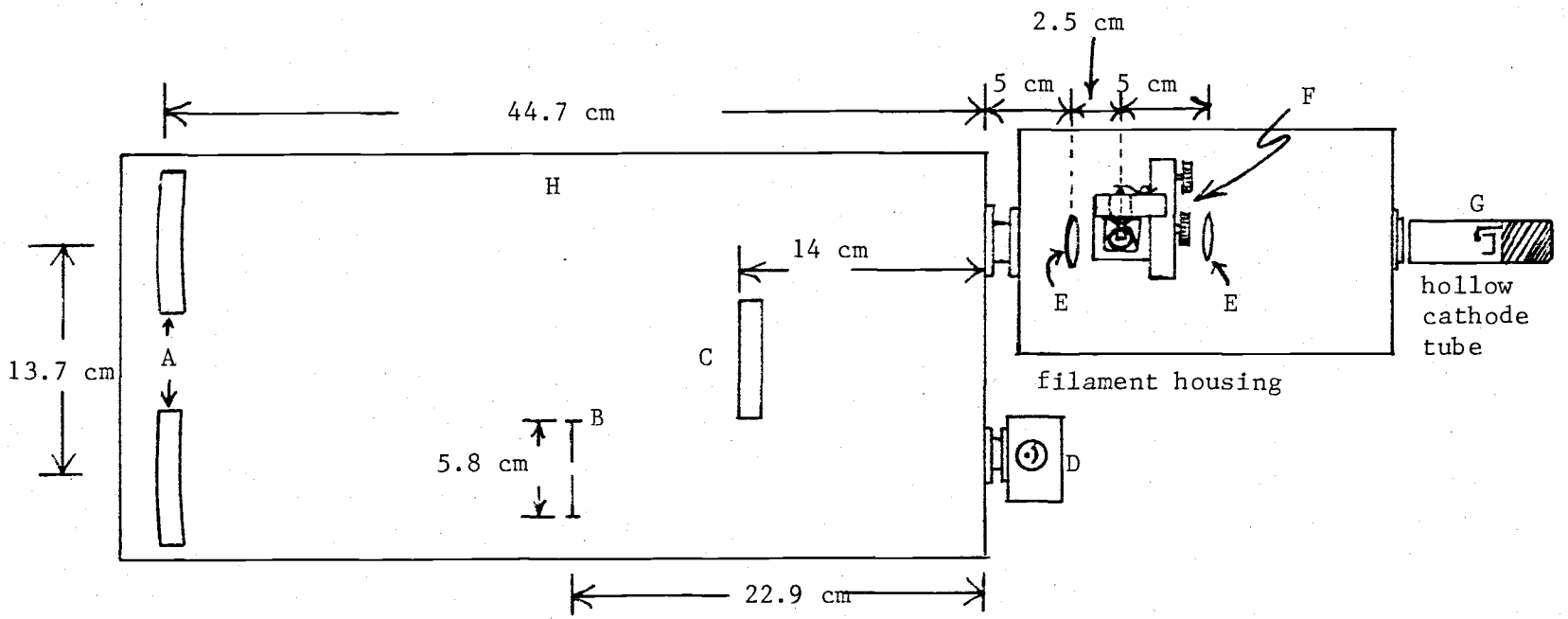

Figure 2. Optical system.

A. 3-inch mirrors
B. 3-4 mm aperture
C. 4.75 x 4.75 cm grating
D. RCA 1P28 photomultiplier tube
E. 5 cm f.l. 1 inch diameter quartz lens
F. X-Y optical bench
G. Hollow cathode lamp
H. MP-1018 monochromator

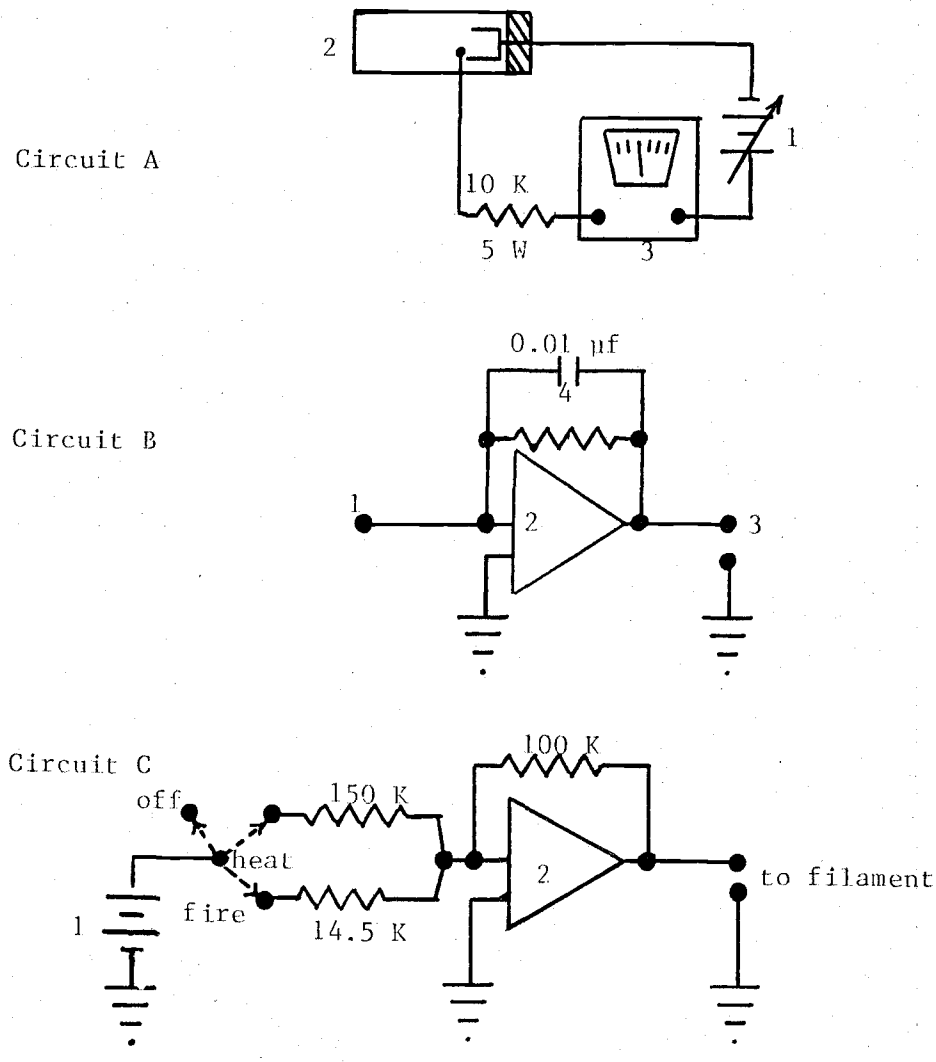

Figure 3. Preliminary electronics.

A. Hollow cathode circuit
   1. Source power supply
   2. Hollow cathode lamp
   3. 0-20 mA d.c. current meter

B. Current-to-voltage converter
   1. BNC to photomultiplier tube
   2. MP-1031 chopper stabilized operational amplifier
   3. Output to a servo recorder
   4. MP-1009 high impedance selector; $10^6\Omega$

C. Filament power source circuit
   1. MP-1008 millivolt source 0-1 V
   2. MP-1026 potentiostat/regulated power supply (a high current operational amplifier)

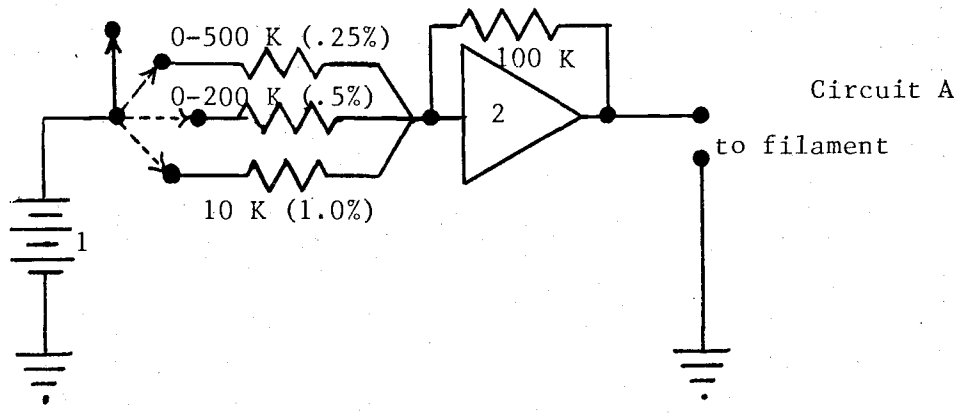

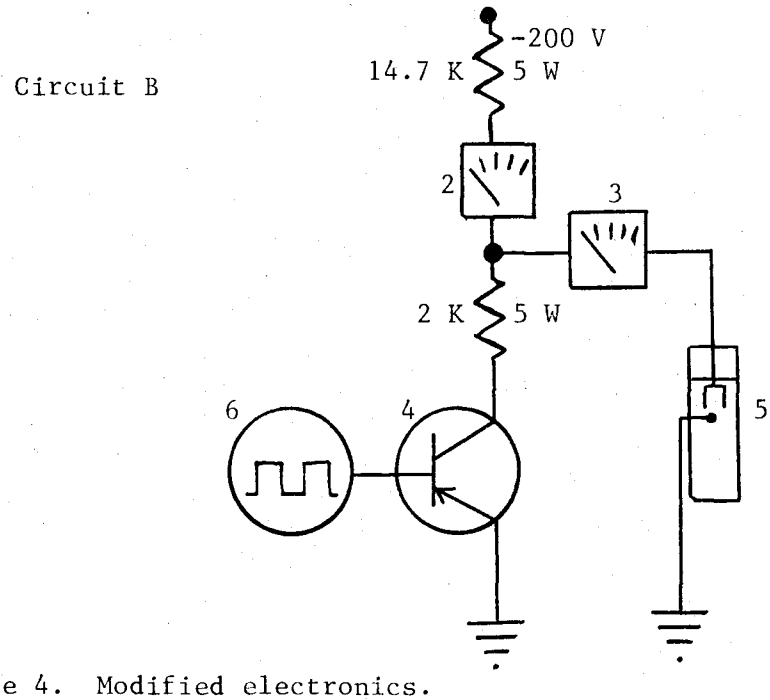

Figure 4. Modified electronics.

A. Filament power source circuit
1. MP-1008 millivolt source 0-1 V
2. MP-1026 potentiostat/regulated power supply

B. Hollow cathode pulsing circuit
1. Source power supply
2. 0-100 ma current meter
3. 0-20 ma current meter
4. High voltage transistor
5. Hollow cathode lamp
6. Square wave generator

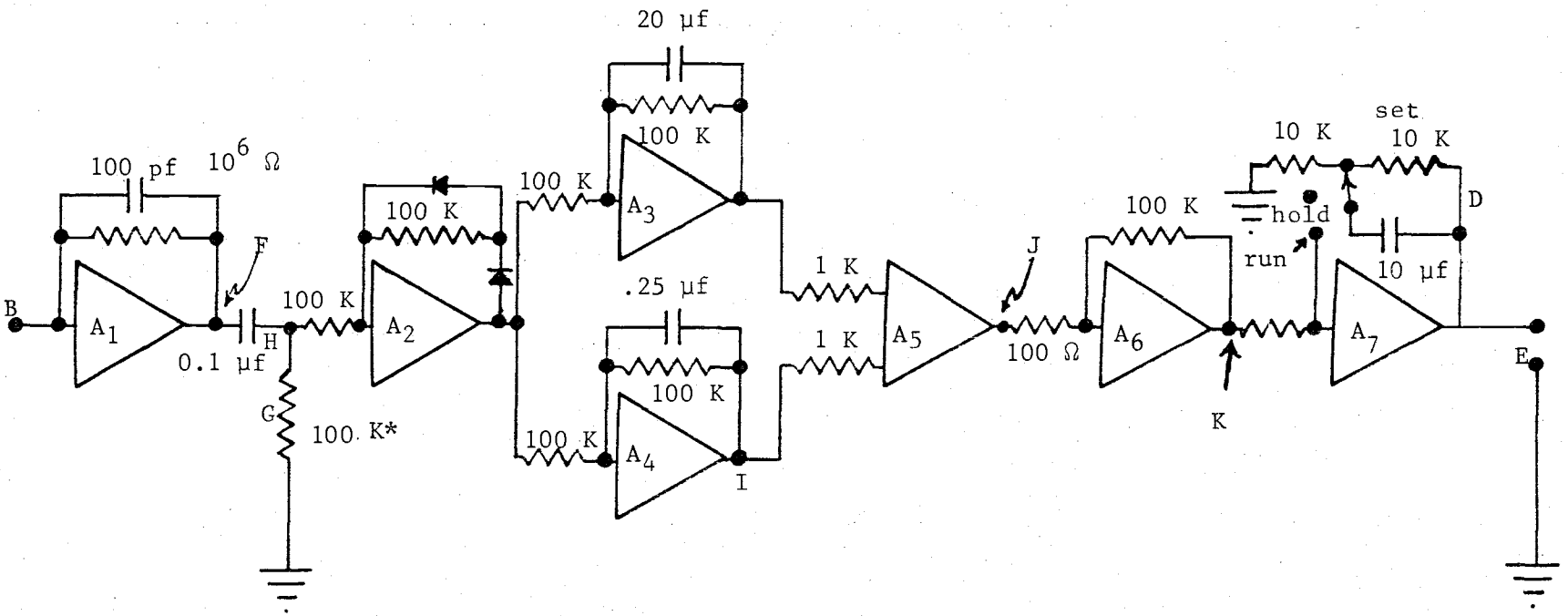

Figure 5. Final analytical signal processing circuit.

A. Amplifiers
   1. MP-1031 chopper stabilized operational amplifier
   2. MP-1006A operational amplifier
   3. MP-1039 dual F.E.T. operational amplifier
   4. MP-1039 dual F.E.T. operational amplifier
   5. MP-1004A log ratio amplifier
   6. MP-1006A operational amplifier
   7. MP-1006A operational amplifier

B. BNC to 1P28 RCA photomultiplier tube
C. MP-1009 high impedance selector
D. MP-1012 integrator
E. To Heath EUW-20 servo recorder

* All resistors are 1% precision.

TABLE III. INSTRUMENTATION.

Item	Type and description	Company and location
Excitation sources	Mg, Cu, Ag and Ca hollow cathode lamps with high spectral output	Westinghouse Corp., Pittsburgh, Pennsylvania
High voltage transistor	Delco 7223 pnp transistor	
Source power supply	Model EUW-15 universal power supply	Heath, Benton Harbor, Michigan
Recording devices	Model EUW-20 strip chart recorder; balance time = 0.1 sec./inch	Heath
	PDP-11/20 16 bit, 8K core; A/D: AD01-D, 10 bit digitization 0-1.25-V scale	Digital Equipment Corp., Maynard, Massachusetts
Monochromator	MP-1018 f/8 grating 4.75 x 4.75 cm; 590 lines/mm recip. line dispersion 35 Å/mm 400 nm blaze; spectral band-pass: 0.70 nm for Ag, Cu and Mg and 0.35 nm for Ca	McKee Pedersen Instruments, Danville, California
Filament power supply	MP-1026 potentiostat/regulated power supply	McKee Pedersen Instruments
Input voltage source	MP-1008 millivolt source	McKee Pedersen Instruments
Signal processing amplifiers	MP-1031 chopper stabilized operational amplifiers	McKee Pedersen Instruments
	MP-1006A operational amplifiers	

TABLE III. (Continued)

Item	Type and description	Company and location
	MP-1039 dual F.E.T. operational amplifiers	
	MP-1004A log-ratio amplifier	
	MP-1009 high impedance selector	
	MP-1012 integrator	
Resistors and capacitors	MP-1014 precision resistor set	McKee Pedersen Instruments
	MP-1028 capacitor set	
Detector	Type 1P28 photomultiplier tube	RCA Electronic Components, Harrison, New Jersey
Photomultiplier power supply	Model 20719 high voltage supply	PRL Electronics Inc., Rahway, New Jersey
Square wave generator	PACO Model E310 sine-square wave signal generator	Precision Apparatus, Inc., Glendale, New York

Since atomization occurred when the filament was heated to incandescence, the helix had to be protected from exposure to air to avoid burn-out. Protection was accomplished by placing the filament in a quartz tube (Figure 1, part F) through which a laminar flow of argon was passed. A plexiglass filament support (part K) prohibited air from entering through the hole where the filament supports protruded through the quartz tube and kept the helix positioned in the center of the tube. Electrical connections were made through wires E_1 and E_2 which were connected to the lamp flange (part J) and lamp base connector.

The lamp could be replaced easily. First, the quartz tube (part F) was removed by moving the plexiglass tube mounting bracket (part G) away from the filament, exposing the helix, and by loosening the quartz tube set screw (part H). Next the protector (part K) and screw from the base electrical connector (part E_2) was removed. The lamp was replaced and the above procedure reversed. The total time for replacement and optical realignment was approximately five minutes.

B. The Optical System

The optical system for these studies is shown in Figure 2. The original burner housing was modified by replacing the nebulizer-burner with the optical bench assembly of Figure 1 and with the necessary lenses and apertures.

The hollow cathode beam was focussed by a 5.0-cm focal length, 2.54-cm diameter quartz lens so that the greatest possible intensity

was found inside the helix. After the beam had passed through the helix, it was focussed onto the entrance slit of the monochromator by a 5.0-cm focal length, 2.54-cm diameter lens. With proper adjustment of this second lens a sharp image of the filament helix could be observed at the exit slit of the monochromator.

The filament was focussed visually at a wavelength of about 580 nm. The filament was adjusted by means of knobs (Figure 1, part C) on the optical bench so that its image could be centered at the exit slit. Since most resonance lines studied here are in the 320-440 nm region, a three-percent decrease in the distance between each lens was made to compensate for changes in focal length due to chromatic aberration. After the initial alignment, the lenses were screwed into place and no attempt was made to relocate the images for various wavelengths used. The entire optical system always remained in the same position.

An aperture was placed nine inches from the exit slit inside the monochromator to allow the viewing of specific volume elements inside the helix and to prevent direct viewing of the filament (see Figure 2, part B). Since the sharp image of the filament could be seen at the exit slit, the aperture could be visually adjusted in order to block out the direct viewing of the glowing tungsten. This helped to reduce the tungsten blackbody emission signal and allowed the photomultiplier to view only the atom population inside the helix.

C. The Electronics

In this project, two different electronic systems were used. Figure 3 illustrates the relatively simple circuitry that was used in the first part of the project, while Figures 4 and 5 illustrate the more sophisticated electronics used in the latter part of the study.

Preliminary Electronics

The hollow cathode lamps were powered at 10-15 mA with the circuitry shown in Figure 3A. The current produced by the photomultiplier tube was processed by a simple current-to-voltage converter with a time constant of 0.01 second (see Figure 3B), and the resulting analytical signal was monitored on a strip chart recorder. Figure 3C indicates the switching circuitry (using a make-before-break switch) used to power the filament. The circuitry used here was designed for intensity measurement only and involved no extra signal correcting electronics. The hollow cathode signal was purely d.c., unlike the later electronics which used a modulated signal for tungsten blackbody emission correction.

The operational amplifier-power supply was used to bias the filament with a predetermined voltage. The input voltage was set to about 1.00 V, and the fixed input resistors were changed to bias the filament at 0.40-1.00 V (to dry) and 6.00 V (to fire), and hence, heat the filament to different temperatures.

Final Electronics

The filament power source was later modified as shown in Figure 4A to include an additional switch position (input resistor, 0-500 K) for an ashing process. The input resistors for drying and firing were replaced by ten-turn potentiometers to provide variable drying, ashing and firing temperatures.

To discriminate against the tungsten blackbody emission that impinged on the slit of the monochromator during the firing step, a modulated hollow cathode lamp coupled with an a.c. amplifier detection circuit (Figure 5) was used.

The hollow cathode lamp was modulated by using the circuit shown in Figure 4B. The circuit is quite similar to Figure 3B except for the addition of the high voltage transistor in parallel with the lamp. As the transistor was switched on by the square wave signal applied to the base, one side of the 2-K resistor became grounded forming a voltage divider which reduced the voltage across the lamp to less than 24 V. This voltage was insufficient to keep the lamp on. When the transistor turned off, the voltage divider was eliminated and the entire voltage was applied to the lamp, turning it on again.

Figure 6A shows the normal total intensity signal observed at point F in Figure 5 (after the current-to-voltage converter circuit, amplifier A_1), plotted on the abscissa as a function of time without

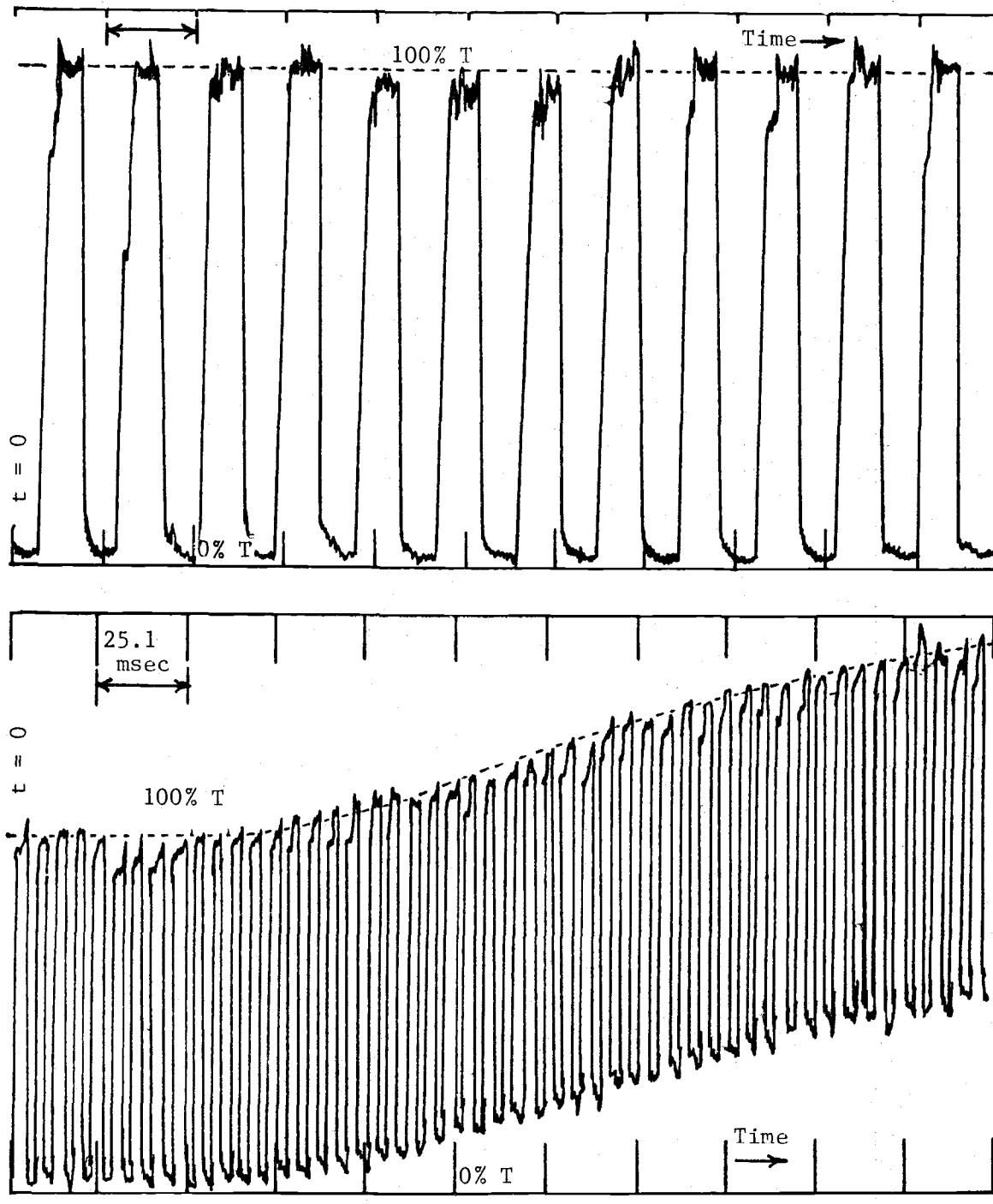

Figure 6. Effect of tungsten blackbody emission on the modulated signal seen at point F in Figure 5 using 2 µl of 0.6 ppm Cu modulation frequency: 182 Hz. Data was collected at a rate of 100 data points per division.
A. Unaffected signal
B. Signal with tungsten blackbody emission present

any atomic absorption or tungsten emission present. However, when the filament was fired the total intensity signal looked like that shown in Figure 6B (note the change in time scale). The rise in the modulated signal baseline was due to the continuum blackbody emission from the tungsten filament. When a sample was atomized the modulated component of the total intensity signal showed a dip due to atomic absorption, as shown in Figure 7A.

The circuit shown in Figure 5 was used to provide a final readout signal using the output of the photomultiplier at point B. First, the high pass filter (resistor G and capacitor H) between amplifiers A_1 and A_2 essentially eliminated the tungsten blackbody emission signal which is low frequency in nature. Amplifier A_2 then rectified this signal to provide a unidirectional signal with the result shown in Figure 7B.

Secondly, amplifier A_4 smoothed this unidirectional square wave signal into a d.c. signal which could be monitored at point I by a very fast recorder or computer interface. An example of a typical atomization run monitored at point I by the computer and later plotted on an oscilloscope or computer display screen is shown in Figure 8A. This figure as well as Figures 6 and 7 plot the output signal versus time. Data points were collected and stored in the computer at predetermined intervals which gave the best visual presentation. Signal inputs ranged from 0.75-1.25 V, which corresponded to 100 percent transmittance. The computer was programmed to expand

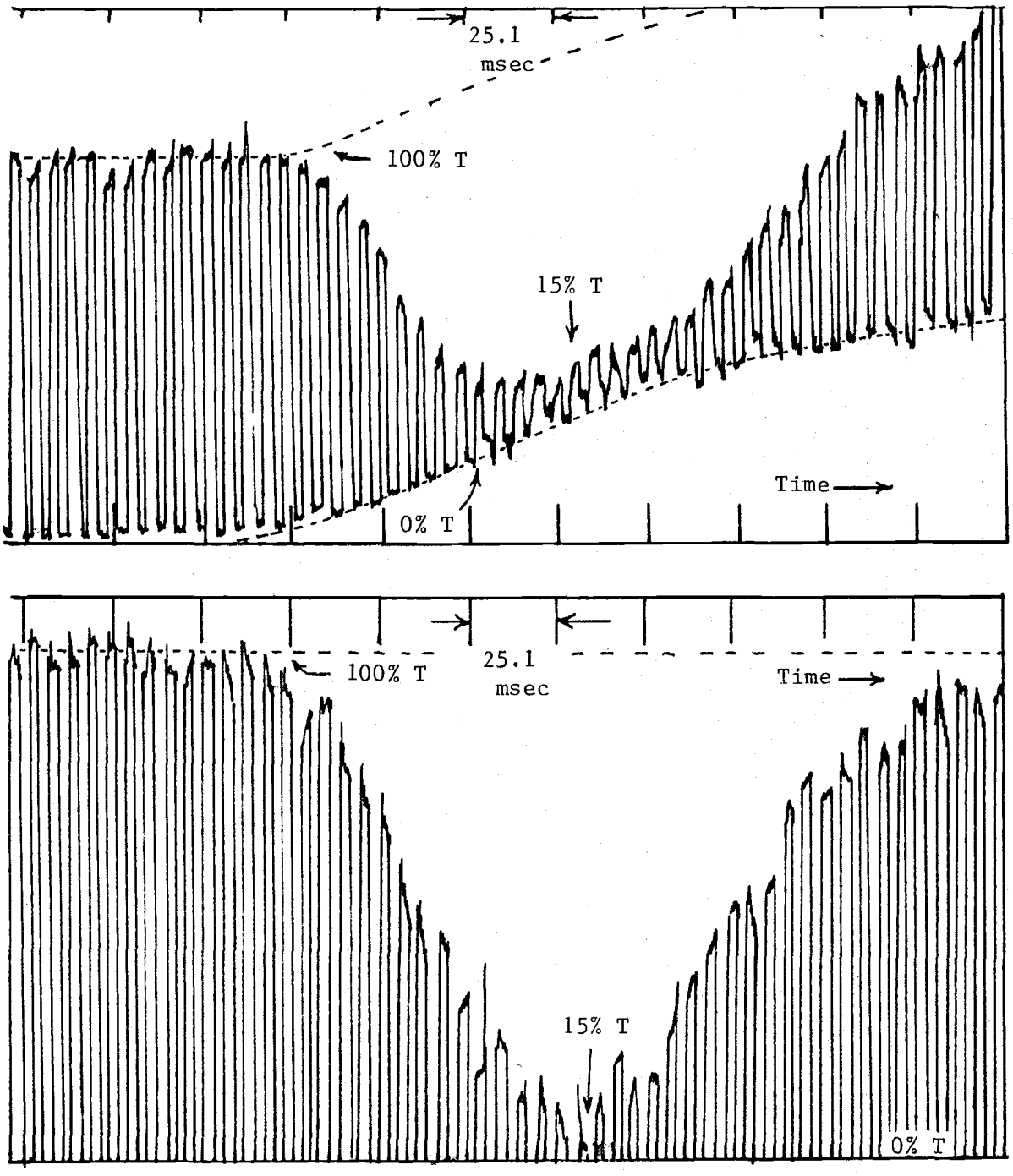

Figure 7. Copper absorption peaks illustrating the elimination of the tungsten blackbody low frequency emission at 324.8 nm.

A. Absorption signal monitored at point F in Figure 5

B. Absorption signal after a.c. filter monitored at the output of amplifier A_2 in Figure 5

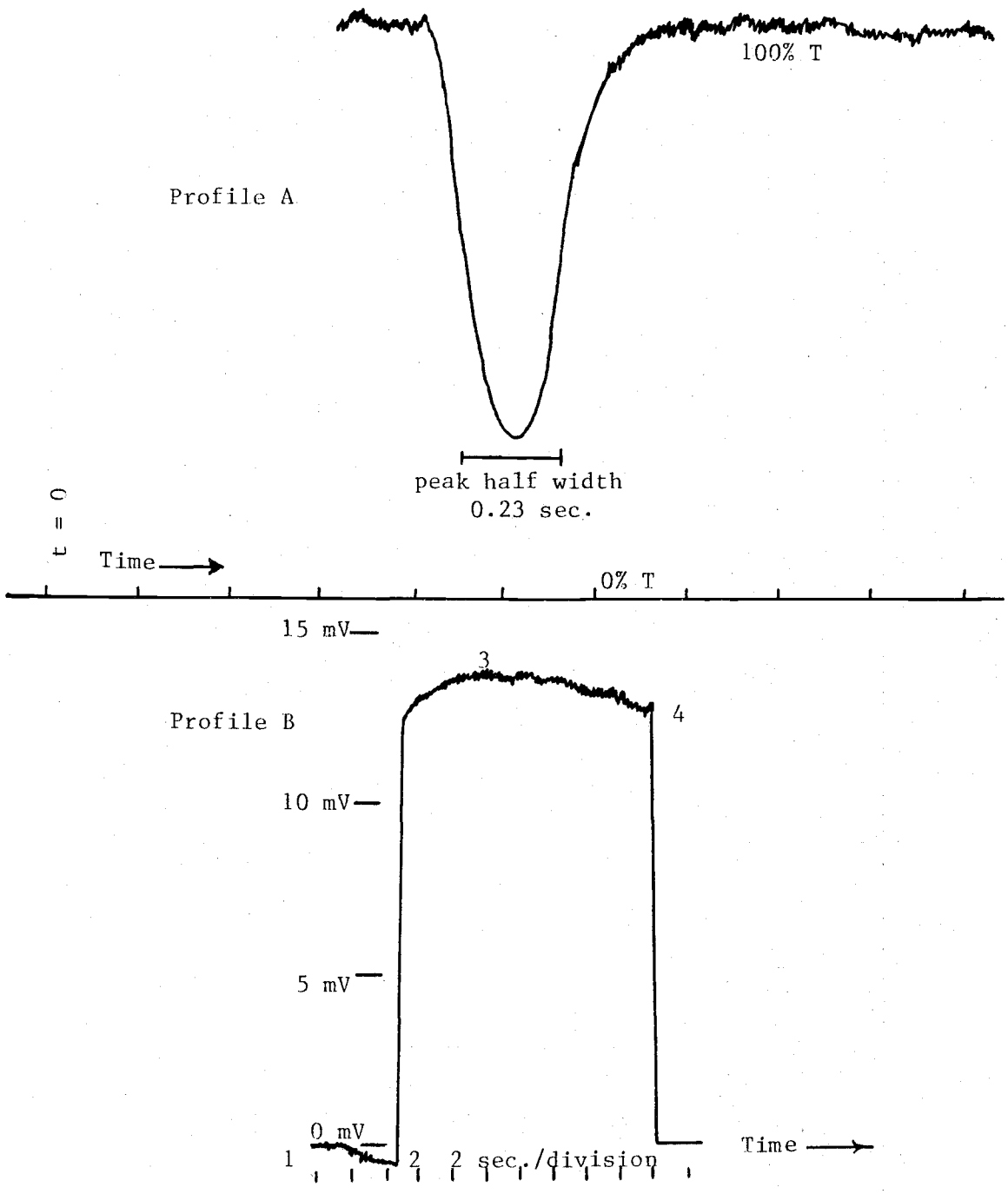

Figure 8. Absorbance and integration signals using 1.2 ng (2 µl of 0.6 ppm) Ag monitored at 328.1 nm.

A. Output seen at point I in Figure 5 where the amplifier A4 time constant is 0.05 sec. Peak indicates percent transmittance profile.

B. Integration signal at point E in Figure 5
   1. Integrator turned on
   2. Atomization initiated
   3. Final peak integration value
   4. Integrator reset

any 100 percent transmittance input signal to the full size of the computer display screen.

Thirdly, a log-ratio transformation was performed by amplifiers A_3, A_4 and A_5 to provide a signal proportional to absorbance at point J. The signal from amplifier A_2 was sent to both amplifiers A_3 and A_4, which provided low pass filter time constants of 2.0 seconds and 0.025 second, respectively. These two signals were then sent through the log-ratio amplifier (amplifier A_5). Since before atomization these two signals are identical except for a slight a.c. ripple difference, the signal at point J looks like a small a.c. signal on top of a zero d.c. level (zero absorbance units). Because of the difference in time constants of amplifiers A_3 and A_4, the output of A_4 followed closely the change in transmittance that occurred during an atomization peak, while the output of amplifier A_3 changed only slightly during an atomization peak. Thus, the output of A_3 served as the reference or 100 percent transmittance signal for log-ratio amplifier A_5 which provides a voltage proportional to the absorbance. The use of the amplifier output voltage at A_3 rather than a constant voltage compensates for drift in the intensity of the hollow cathode lamp and photomultiplier voltage.

The time constants were selected to minimize both noise and peak height errors as well as to convert the modulated hollow cathode signal into a purely d.c. signal. McWilliam and Bolton (17) have provided equations indicating that, for the 0.025-second time constants used in amplifier A_4 (Figure 5), normal peaks having half-height

widths greater than 0.20 second have peak absorbance values no less than 98 percent of the true value. Similar calculations indicated that amplifier A_3 with a time constant of 2.0 seconds gave a reduction in the 100 percent transmittance signal of about 2.5 percent at the peak of the absorption profile. This signal provided the log-amplifier A_5 with an adequate reference signal.

Since this reference signal changed a small amount during the peak profile, a certain amount of distortion occurred at point J. A slight skewing toward increased time values and a slight peak broadening was found. However, absorbance peak profile distortions are minimal and reproducible. This absorbance peak (not to be confused with the transmittance peak obtained at point I) was then passed through amplifier A_6 and then into the integrator A_7. A sample of the resulting integrated signal seen at point E is shown in Figure 8B.

III. PROCEDURE

A. Solution Preparation

Standard solutions were prepared by dilution of the stock solutions shown in Table IV. All solutions were prepared with doubly distilled water and were stored in polyethylene containers. For calcium analysis the doubly distilled water was also passed through an ion-exchange column containing Dowex 50W-X4. This reduced the calcium concentration in the water to about 2.0 ppb (4 pg in 2 µl) which is close to the calcium detection limit observed in this study. Precautions were taken to minimize exposure of the solutions to room light. To circumvent stability difficuities all standard solutions were analyzed within ten minutes of preparation.

B. Analysis Procedure

The instrumentation was allowed to warm up at least 45 minutes before use. Several minutes prior to analysis the argon flow was turned on to purge the filament enclosure. Then the filament power source was switched to the "fire" position to clean impurities off the tungsten filament surface. The sampling and atomization procedures for the vertical and horizontal filament positions are described below. After atomization, the filament supply was left in the "fire" position to clean off remaining sample and impurities.

TABLE IV. REAGENTS.

Desired solution	Material used	Diluted to
1000 ppm magnesium	16.725 grams of magnesium chloride hexahydrate	2 liters
1000 ppm copper	5.366 grams of copper chloride dihydrate	2 liters
1000 ppm silver	3.150 grams of silver nitrate	2 liters
1000 ppm calcium	2.726 grams of calcium chloride dihydrate	1 liter
1000 ppm phosphate	1.453 grams of potassium dihydrogen phosphate	1 liter

Vertical Filament

For the early work with the filament in the vertical position the sampling procedure was basically that described by Williams and Piepmeier (16). The progress of the drying could not be monitored directly, i.e., one did not know exactly when the solvent had been completely boiled off. Therefore, each sample was dried for a specified amount of time (usually 30 seconds).

Horizontal Filament

For the later work in which the filament was in the horizontal position, the procedure was modified due to the more sophisticated electronics and the unique characteristics of the filament in this new position. First it was noted that with the horizontal filament position, the intensity signal at point F in Figure 5 was an excellent indicator of the drying process. When the sample droplet was suspended inside the helix, virtually all of the hollow cathode light viewed by the photomultiplier tube in the absence of the droplet was diverted by the droplet so that the output signal at point F, viewed on an oscilloscope is zero (zero percent transmittance). Emission from the filament was negligible during the drying process.

The signal remained at this level until approximately 75 percent of the water had been evaporated. The signal then fluctuated between 30 and 80 percent transmittance for several seconds and then abruptly returned to 100 percent transmittance. At this point nearly

all of the water was gone and the remaining amount was evaporated within seconds. The total drying time was 15-20 seconds.

The horizontal filament was then heated at 1.50-2.00 V after the drying process in an "ashing" or "prefire" process by means of the additional switch position (0-200 K) shown in Figure 4B. This intermediate step helped to eliminate light scattering and unwanted absorption (molecular absorption) at the time of atomization. This scattering resulted in the double peaks similar to those seen by Williams and Piepmeier (16). The recording devices were activated (t = 0 in Figures 6, 7 and 8) and the sample was atomized when the signal at point J (as indicated by an oscilloscope) returned to zero volts (or 100 percent transmittance). The length of the "ashing" period was partly determined by the time necessary for the 20-μf capacitor in amplifier A_3 to charge up to its 100 percent transmittance level. In order to facilitate the recording process, the integrate or "run" switch on amplifier A_7 was incorporated into the filament power source switch. Thus, when the power source switch was turned to "fire," the integrator started to integrate the signal seen at point K. The integrator recorded any deviation from zero absorbance. A recorder at point E recorded the integral of the absorbance over the entire absorption peak. In most cases the transmittance was monitored at point I by either a storage oscilloscope or by the computer so that peak shape and noise levels could be observed.

IV. RESULTS AND DISCUSSION

A. Choice of Experimental Variables

A number of the experimental variables shown in Table V were found to influence the analytical results of the horizontal filament. Values used for the vertical filament study performed here are also given. In order to improve the analytical results a general study of some of the influences of the variables was performed. This study also showed which variables are critically important to be considered in a later optimization study. A true optimization program would have optimized each variable while all other variables were set to their optimum values. This would involve a big trial and error procedure since changing one variable may change the optimum value of another variable. Such a study is beyond the scope of this thesis and could be taken up in later work, perhaps for a Ph.D. thesis.

The variables discussed here were adjusted to that value which yielded the lowest relative standard deviation, σ_{rel} of the average peak absorbance value. Unless otherwise stated, standard deviations were calculated from four replicate sample runs.

Easily Adjusted Variables

The variables first studied were those whose best value seemed rather obvious or where only a short study seemed necessary. These included:

TABLE V. SYSTEM VARIABLES FOR VERTICAL AND HORIZONTAL FILAMENT STUDIES.

Variable	Value using vertical filament	Value using horizontal filament
Modulation frequency	--	200 Hz
Hollow cathode lamp r.m.s. current	7 mA	15 mA
High pass filter cutoff frequency	--	15.9 Hz
Argon flow rate	7.5 l/min.	1 l/min.
Filament voltages:		
Dry	1.00 V	1.00 V (150°C)
Prefire	--	2.00 V (1300° ± 30°C)
Fire	4.00 V	6.00 V (2000° ± 15°C)
Sample size	2 µl	2 µl
Monochromator slits:		
for Mg, Cu and Ag	50 µ	50 µ
for Ca	--	25 µ
Hollow cathode beam location	1 mm above top of filament	bottom ¼ of inside filament (position 1)

1. modulation frequency and high pass filter cutoff frequency;
2. hollow cathode lamp current;
3. sample size;
4. drying voltage; and
5. standard solution storage time.

1. Modulation and High Pass Filter Cutoff Frequency

Modulation frequency was found to have little influence on the relative standard deviation over the range of about 50 Hz to 220 Hz. A high modulation frequency would be best for short absorption pulses. However, frequencies greater than 220 Hz cannot be used because the hollow cathode lamp does not completely switch on and off and the baseline becomes nonzero, reducing the analytical absorption signal. The cutoff frequency for the high-pass cutoff filter is important in order to prevent extraneous signals due to the low frequency tungsten emission and baseline drift. It was found that a high-pass filter corner frequency of 16 Hz coupled with a modulation frequency of 200 Hz provided essentially complete discrimination against low frequency components and resulted in essentially all the modulated hollow cathode signal being passed.

2. Hollow Cathode Lamp Current

Modulated lamp currents of 5 mA average current (10 mA, 50 percent duty cycle) and no d.c. background current, within the maximum d.c. current specified by the manufacturer, were used for all hollow cathode

lamps. Interferometer studies (18) have shown that Cu and Ag hollow cathode lamps when modulated with such currents, give narrow emission line profiles with no self reversal.

3. Sample Size

A sample size of 2 µl was used on the horizontal filament because larger droplets tended to disperse outside the helix and adhere to the filament supports. Atomization was less efficient outside the filament, and residues collected there were not easily vaporized. This resulted in "ghosting" effects and significantly larger standard deviations. In the study by Williams and Piepmeier (16), a sample size of 3 µl was used for the vertical filament.

4. Drying Voltage

A drying voltage of 1.00 V was chosen for all elements because it produced the highest temperature for rapid evaporation yet did not cause losses due to spitting or violent boiling.

5. Standard Solution Storage Time

Standard solutions in the low parts-per-million range showed very poor stability, even when stored in polyethylene bottles. Figure 9 shows how absorbance from 2 µl of a 0.2-ppm (0.4 ng in a 2-µl aliquot) Ag solution changed with time. Similar results were obtained from Ca standards. With this in mind, standard solutions were analyzed within ten minutes of preparation.

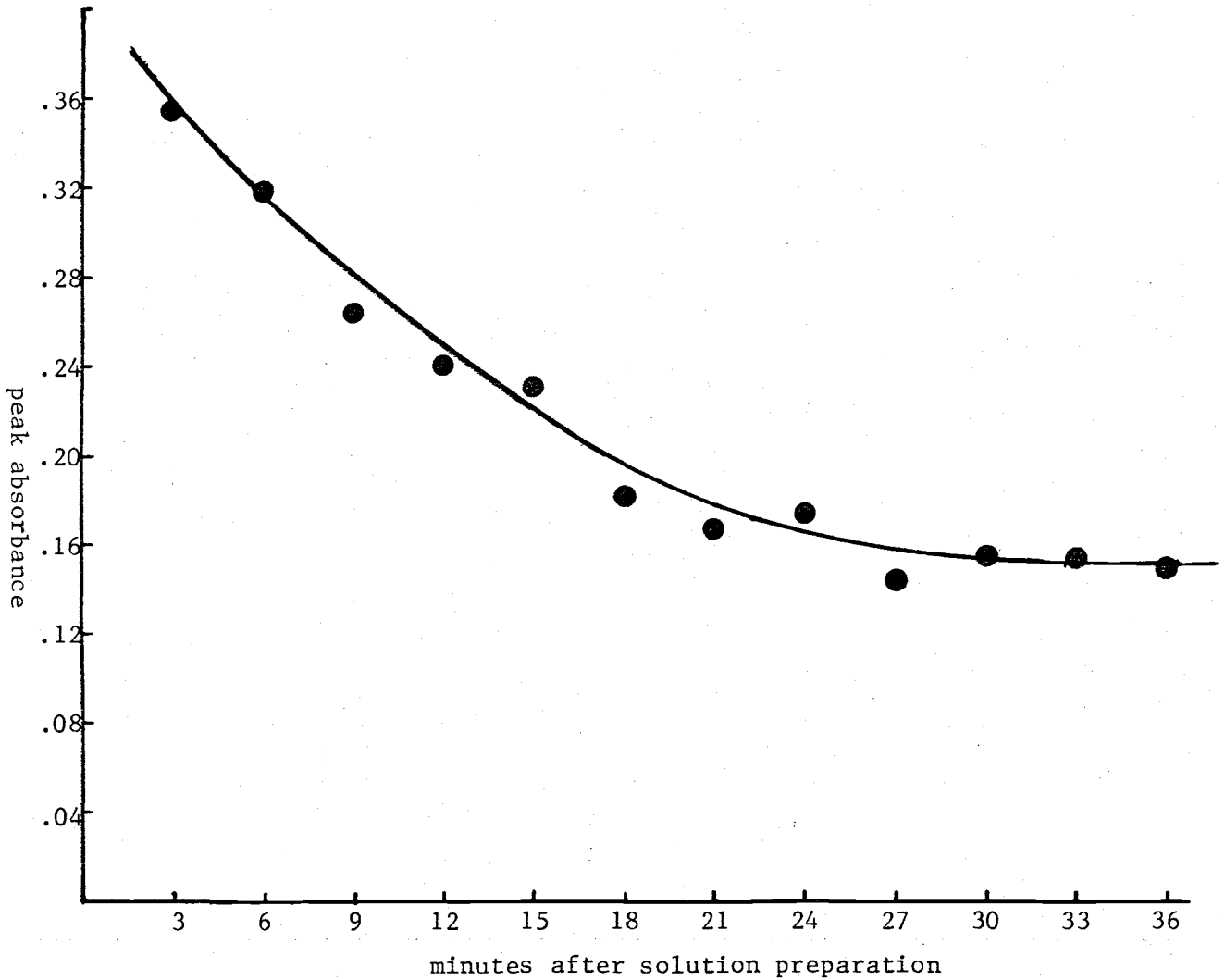

Figure 9. Dependence of peak absorbance on time using 2 µls of 0.2 ppm Ag at 328.1 nm.

Variables Requiring In-depth Study

A number of other variables required more intensive investigation. These proved to have profound effects in such areas as spectral interferences, peak absorbance values, the shape of the analytical curves and relative standard deviations. These variables, by no means a complete list, can be roughly categorized in the following manner. It should be realized that many of these could fall into several categories.

1. Variables influencing σ_{rel}
   a. Aperture size and location
   b. Gas flow rate
2. The variable eliminating double peaks--the "prefire" step
3. Variables influencing peak absorbance values
   a. Firing voltage
   b. Prefire voltage
4. Variables influencing the slope and shape of the analytical curve
   a. Prefire cooling
   b. Vertical and horizontal filament position

1. Variables Influencing σ_{rel}

Aperture Size and Location. Three different locations and two different aperture (Figure 2, part B) diameters were studied. Using an aperture that showed an area with a diameter one-fourth that of the helix inner diameter, the area directly above the bottom, in the middle and directly under the top of the helix were studied to determine which gave the lowest σ_{rel}. Also a larger aperture which allowed the viewing of two-thirds of the total area was studied.

Table VI gives the results of this study. In this case, position 1 gave both the smallest peak absorbance and the best relative standard deviation. This optimum viewing area, using the smaller of the two diameters, was focussed on the region just above the inside bottom of the coils. This is probably where the largest amount of sample was deposited when the solvent was driven off in the drying step. The atomic vapor is viewed immediately after vaporization when diffusion is at a minimum. Therefore, all measurements were made with the aperture allowing only the region shown in Table VI, position 1 or position 4 in the case of low intensity lamps, to be viewed by the photomultiplier.

Smaller viewing areas were found to reduce the photomultiplier output signal to the point where shot and lamp flicker noise became dominant. Larger sizes reduced these two sources of noise, but the standard deviation of replicate samples was disproportionately poorer.

Gas Flow Rate. The argon flow rate was found to be the most sensitive variable to adjust. Figure 10 shows the effect of flow rate on the relative standard deviation of the peak absorbance values. For 0.4 ng (2 µl of 0.2 ppm) Ag samples and a firing voltage of 6.0 V, the peak absorbance and relative standard deviations of four replicate runs were determined at various argon flow rates and plotted to determine the best value. This graph indicates that a much lower flow rate (2 l/min.) than previously used (10 l/min.) for the vertical filament (16) increased sensitivity and improved the reproducibility.

TABLE VI. VIEWING REGION RELATIVE STANDARD DEVIATION STUDY.*

Position	Aperture image	Diameter and location	Absorbance	Standard deviation	Relative standard deviation
1		1/4, bottom	.149	.007	.047
2		1/4, center	.307	.037	.111
3		1/4, top	.409	.048	.118
4		2/3, bottom	.229	.013	.057

* Two microliters of 0.02-ppm Ca was used at a wavelength of 422.7 nm. Values are based on six measurements at each position.

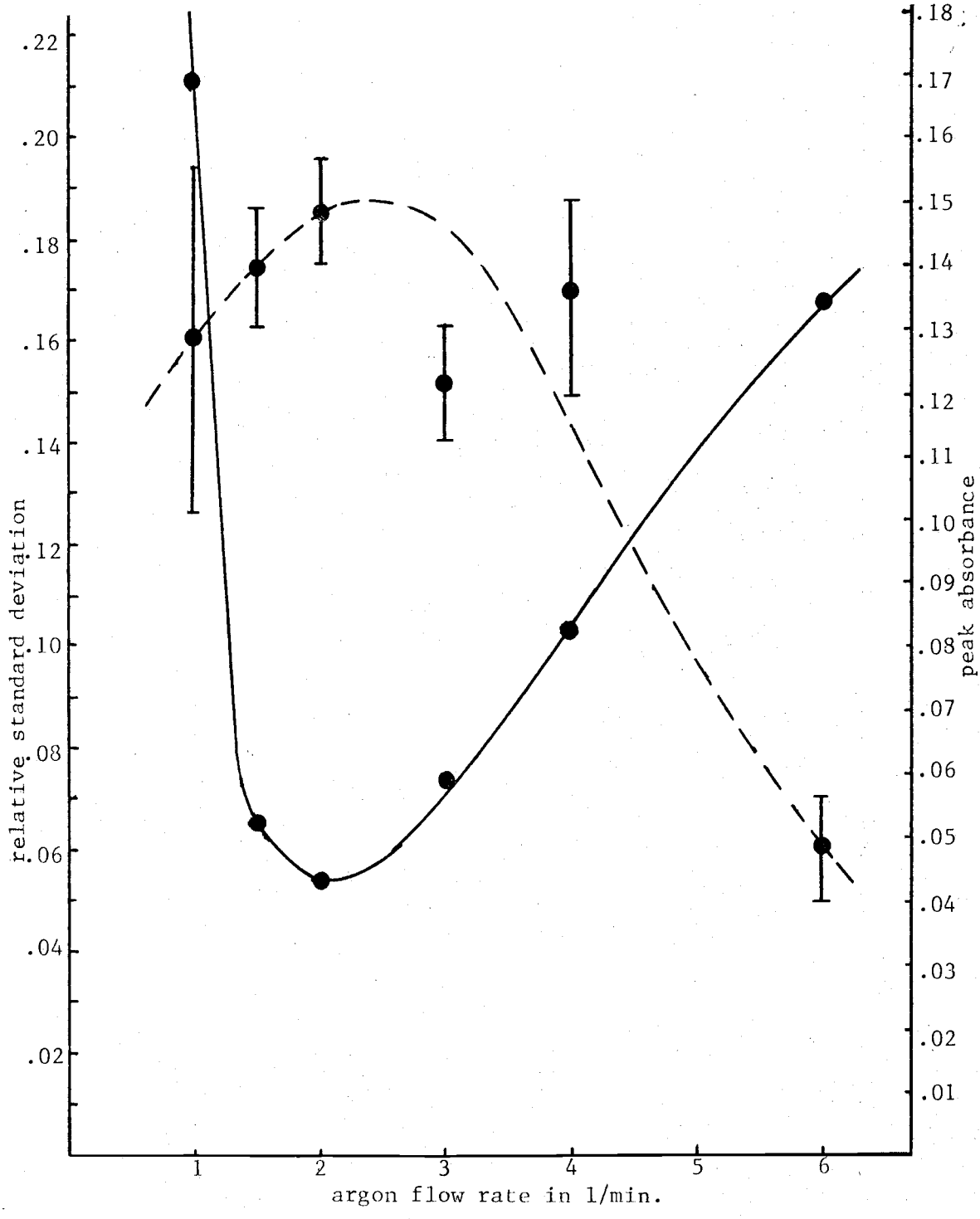

Figure 10. Argon flow rate optimization indicating relative standard deviation (solid line) and peak absorbance values (broken line) versus flow rate. 0.4 ng (2 µl of 0.2 ppm) Ag was used as a sample at 328.1 nm. Error bars indicate plus or minus one standard deviation.

With a lower flow rate than was used in the work by Williams and Piepmeier (16), it was economically feasible to allow the argon to flow continuously, thus eliminating flow rate fluctuations that are caused by turning the gas flow on and off. Ideally, one would like to have no argon gas flow, such as in a sealed chamber filled with argon, so that the atomic vapor remains inside the helix longer. This would result in the highest possible atomic population inside the helix and hence, the highest possible atomic absorption sensitivity. Since this chamber was open-ended, some gas flow had to be present to prevent the incursion of air which led to oxidation of the tungsten. However, at low flow rates the atomic vapor dispersed in an irreproducible manner as indicated in Figure 10 by the large standard deviation obtained at a flow rate of 1 l/min. on the peak absorbance versus flow rate curve. At high flow rates the vapor was swept away faster and the atomic vapor density decreased, resulting in reduced sensitivity, as indicated by the decreasing peak absorbance values obtained at flow rates of 4 and 6 l/min. in Figure 10. At higher flow rates, peak absorbance calibration curves bend toward the concentration axis as illustrated in Figure 11 which shows the peak absorbance calibration curves for Ag at 1.5 and 7.5 l/min. and a 6-V firing voltage. Peak broadening was relatively small at very low analyte quantities (0.08-0.4 ng Ag) as shown in Table VII where the absorbance peak widths of half height are tabulated for several Ag quantities analyzed at a 6-V firing voltage and a 7.5-l/min. flow rate. Any decrease in sensitivity or increase in half-width cannot be readily

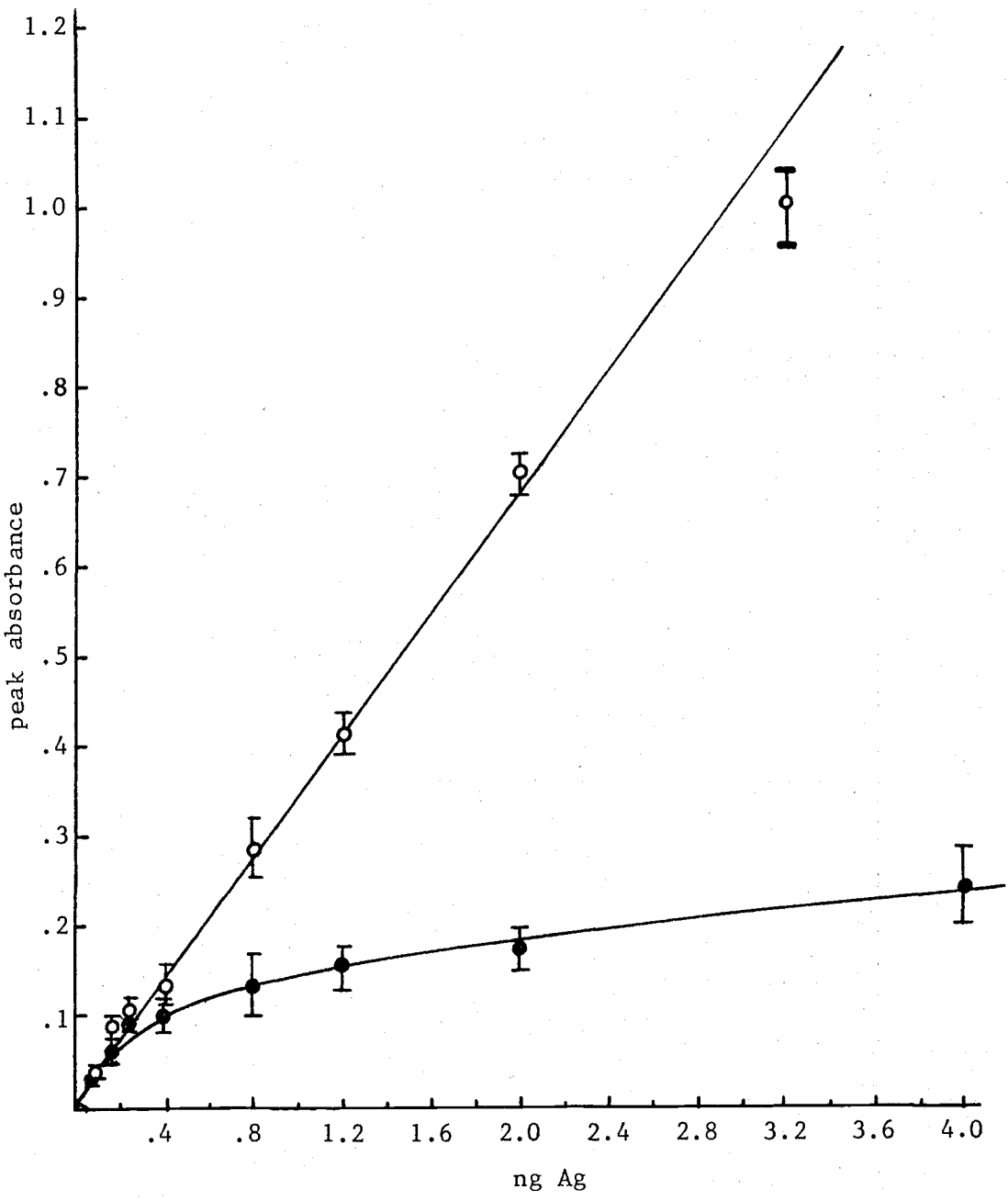

Figure 11. Silver calibration curves at argon flows of 1.5 l/minute (hollow points) and 7.5 l/minute (solid points); wavelength = 328.0 nm. Error bars indicate dispersion of plus or minus one standard deviation based on four to six replicate runs.

TABLE VII. EFFECT OF THE QUANTITY OF SILVER ON ABSORBANCE PEAK HALF-WIDTH AT A HIGH ARGON FLOW RATE.

Quantity of Ag in ng	Absorbance peak half-width in msec	Standard deviation in msec
0.08	18.0	3.0
0.24	17.3	1.3
0.4	22.2	1.6
0.8	59.1	4.4
1.2	69.8	4.2
2.0	81.1	3.7
4.0	98.4	4.7

Analyzed at 328.1 nm with an argon flow rate of 7.5 l/min. and a firing voltage of 6.0 V.

discerned at these low quantities while a significant decrease in sensitivity occurred at higher quantities where broadening increased greatly. Figure 12 plots the absorbance peak integration calibration curves for Ag at the two flow rates mentioned above. This indicates that the slope or sensitivity was less at the higher flow rate but relatively concentration independent, there being a slight curvature at low quantities on the 7.5-l/min. curve. This decrease in the time integrated absorbance sensitivity is primarily caused by analyte density decrease due to increased convection transport and to a cooling effect on the filament and analyte atoms by the flowing gas. The faster rate reduced the temperature of the filament from 2000°C to about 1900°C. The method of measurement of these temperatures will be discussed later.

2. The Variable Eliminating Double Peaks--The "Prefire" Step

A prefire step was added to the precedure to eliminate an interfering peak which was observed on the absorption versus time profiles of Ag, and to a lesser extent, Ca, Cu and Mg. Figure 13 illustrates a typical Ag profile run at a 6.0-V firing voltage and a 2-l/min. flow rate. Two absorption maxima are found where peak 1_a is due to interfering absorption or scattering by some unknown species, and peak 1_b is due to silver absorption. A "prefire" step where 2.00 V is applied to the filament for five seconds followed by a 20-second cooling off period before atomization resulted in absorption peak 2. The shape and size of the analyte absorption

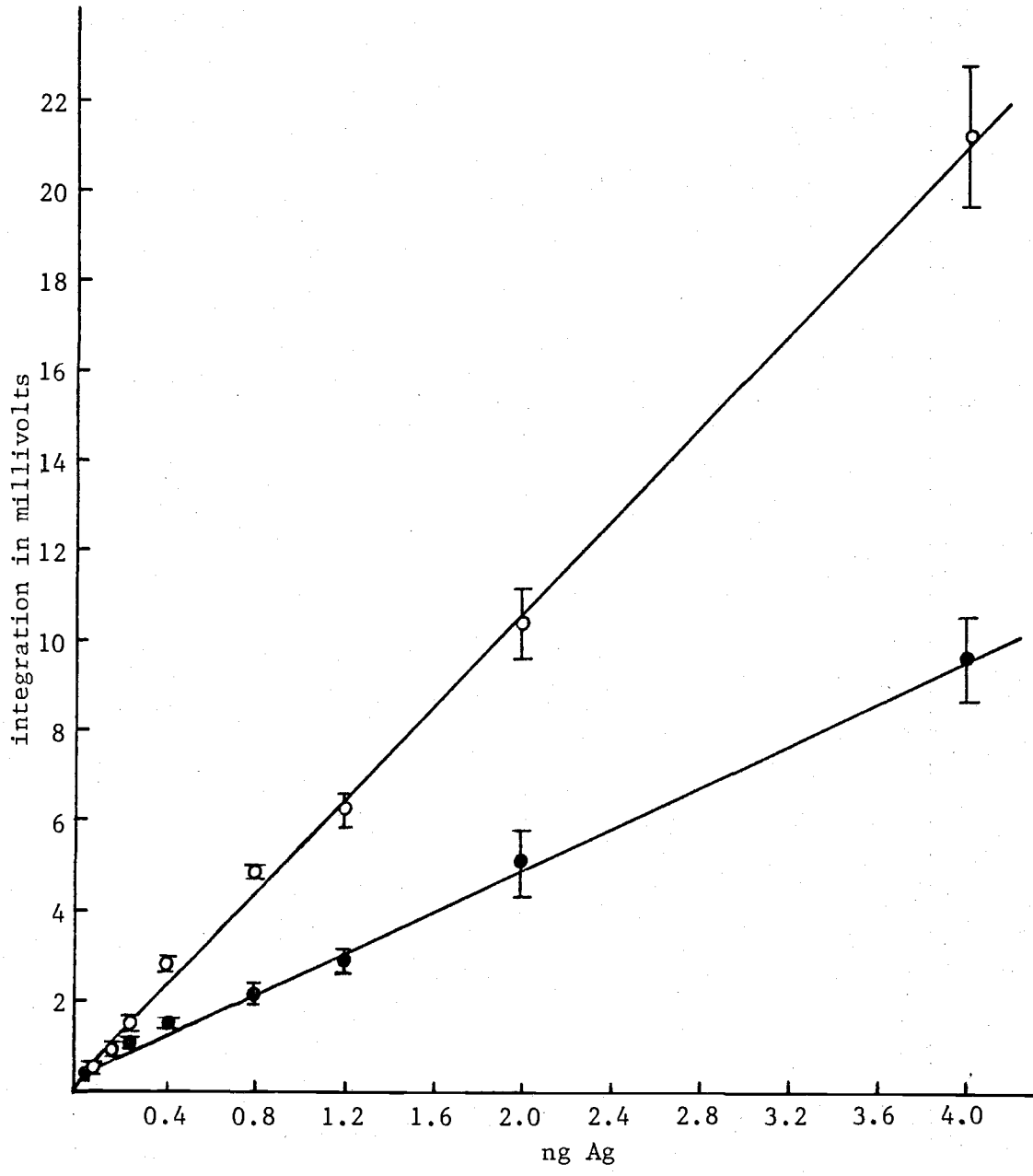

Figure 12. Silver integration calibration curve at argon flows of 1.5 l/minute (open points) and 7.5 l/minute (solid points).

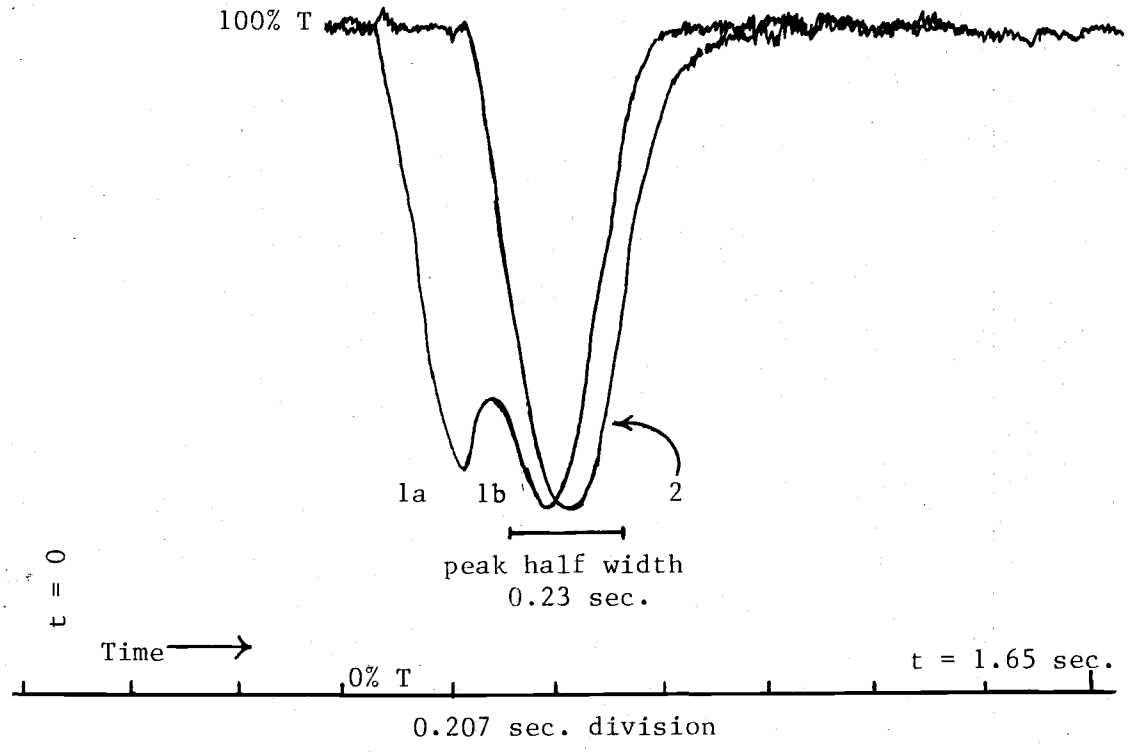

Figure 13. Absorbance signal seen at point I in Figure 5. Peak 1 indicates absorption profile without a prefire step; peak 2, with optimized prefire step.

peak was apparently unaffected by this intermediate step as shown when the curves are superimposed.

Figure 14 shows the absorption profiles of 1.2 ng Ag (2 µl of 0.6 ppm) at two resonance wavelengths, 328.1 and 338.3 nm, respectively. These two wavelengths have analytical sensitivities which differ by a factor of two (19), where the 328.1-nm line is the more sensitive. Therefore, analysis at the 328.1-nm wavelength should yield an absorbance value twice that which was found when analysis was performed at the 338.3-nm line. These two analyte profiles changed as expected when errors due to peak overlap were considered while the first peaks were wavelength independent. This suggested the presence of light scattering by impurities such as water held inside the sample crystal or dust. The impurity peak was not very reproducible and was seen at a non-absorbing resonance line (324.8-nm Cu line), lending credence to this idea.

Similar double peaks for Cu and Mg were seen by Williams and Piepmeier and were attributed to non-homogeneous heating of the filament, since in their case both peaks were observed only at the absorption line.

The value of 2.00 V was chosen for the "prefire" step because it was found to be the highest voltage possible without causing the analyte atoms to vaporize. This will be discussed in more detail at a later time.

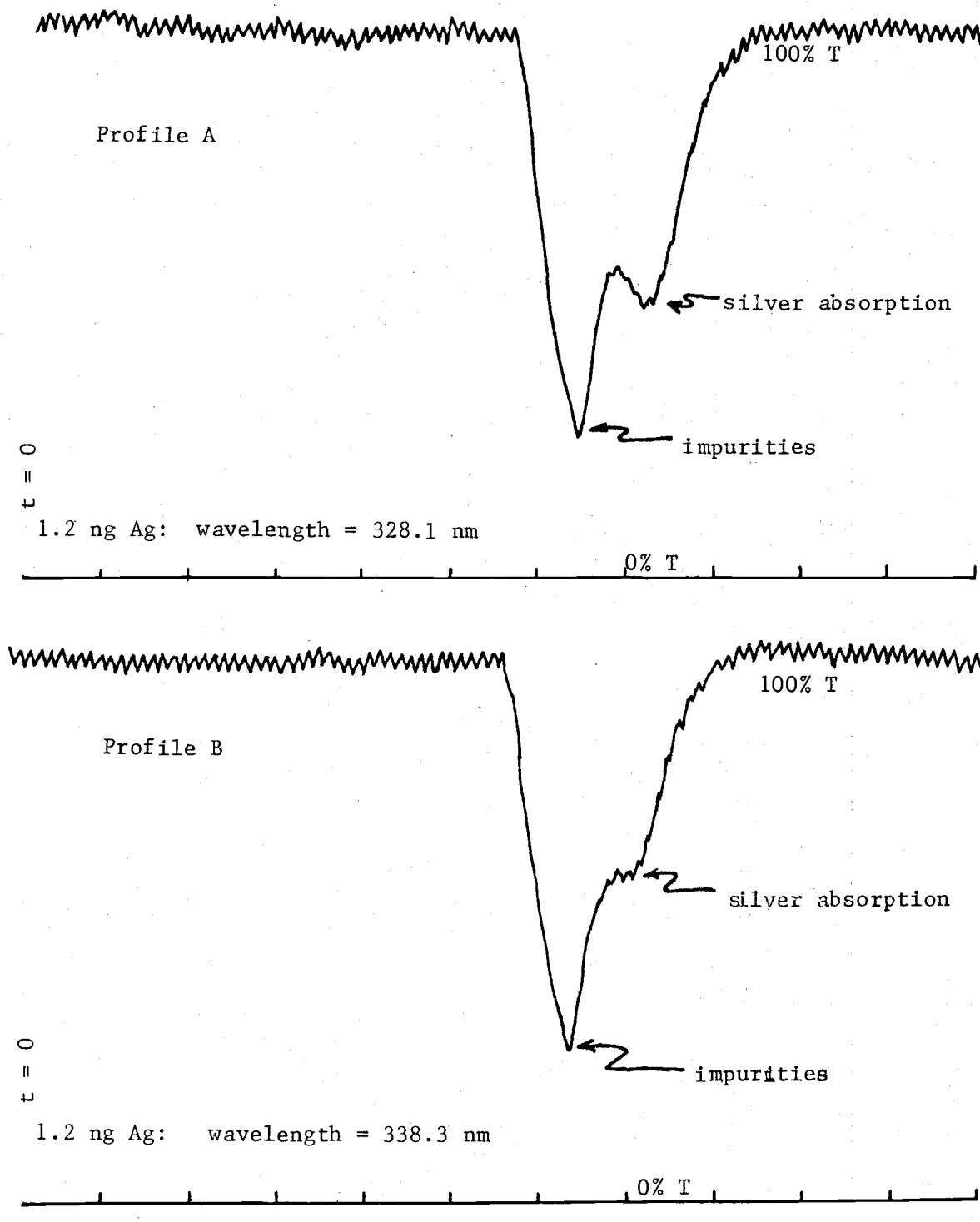

Figure 14. Characteristic shapes of silver absorption peaks with interferences at 328.1 nm and 338.3 nm.

3. Variables Influencing Peak Absorbance Values

Firing Voltage. Fire and prefire (by means of the preatomization filament temperature) voltages were critical since they affected the rate of atomization and, therefore, the peak absorbance value. Figure 15 shows how the firing voltage influenced the relative standard deviation for a 0.12 ng (2 µl of 0.06 ppm) Ca solution analyzed with a 1-V drying voltage, no "prefire" and a 2-l/min. flow rate. Various firing voltages up to 6.0 V are plotted on the abscissa and the corresponding changes in σ_{rel} are plotted on the ordinate. This graph indicates that higher voltages or more efficient atomization temperatures gave better reproducibility. However, voltages above 6.0 V caused oxidation of the tungsten, filament brittleness and frequent burnouts. This voltage provided peak absorbance values with the lowest relative standard deviations, although a voltage of 4.00 V gave the highest peak values as indicated by curve A in Figure 16 where peak absorbance values from the same study are plotted against the various firing voltages. Therefore, a voltage of 6 V was selected as the optimum value for all analyses by providing the highest allowable atomization temperature.

In order to obtain some indication of these filament temperatures, a Leeds and Northrup model 8632-C Optical Pyrometer was used. Measurement of the filament temperatures was made under the experimental conditions listed in Table V. The firing voltage of 6.00 V provided a tungsten surface temperature of 2000 $\pm$ 15°C.

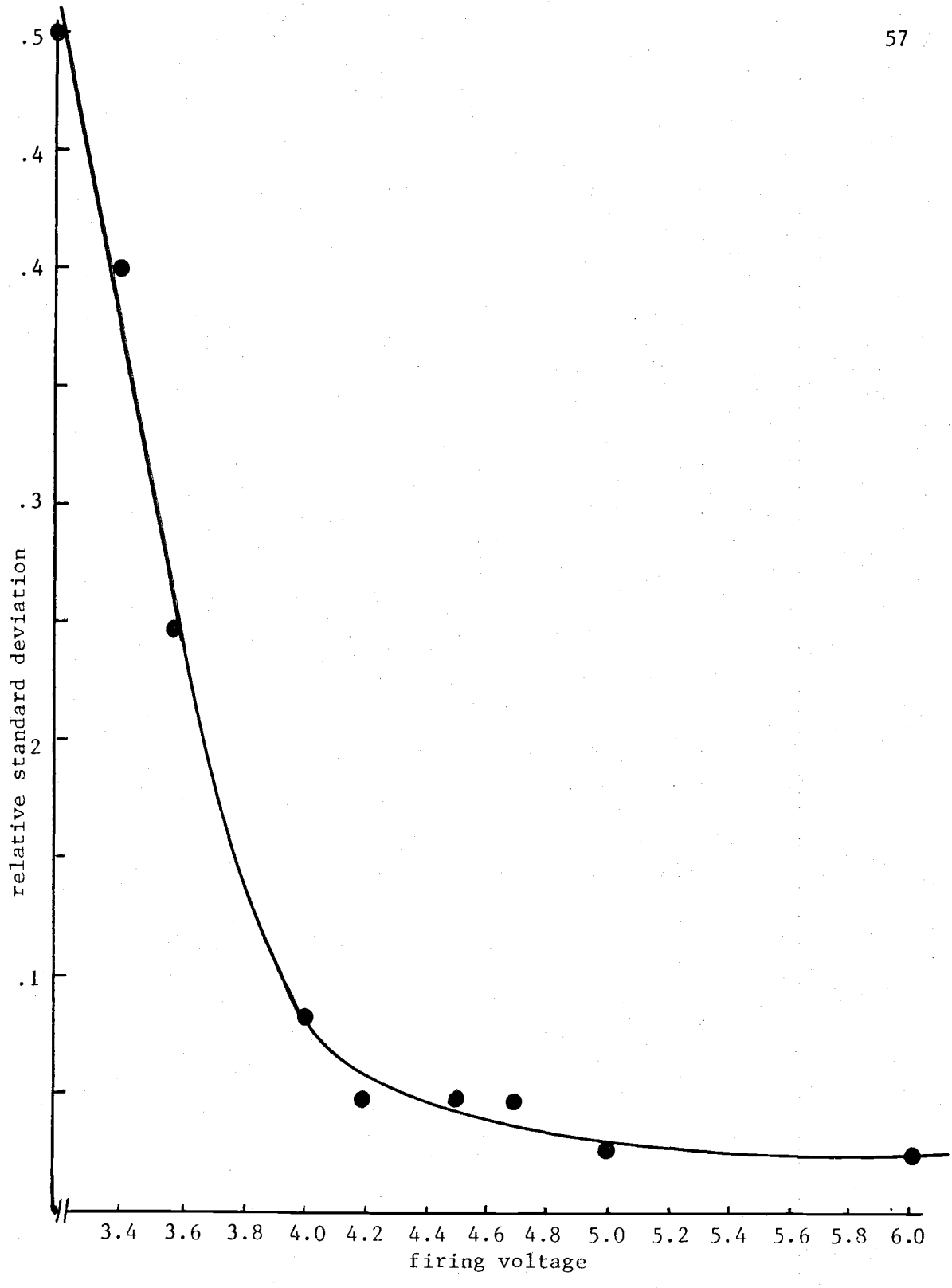

Figure 15. Dependence of peak absorbance relative standard deviation on filament firing voltage using .12 ng (2 µl of 0.06 ppm) Ca at 422.7 nm.

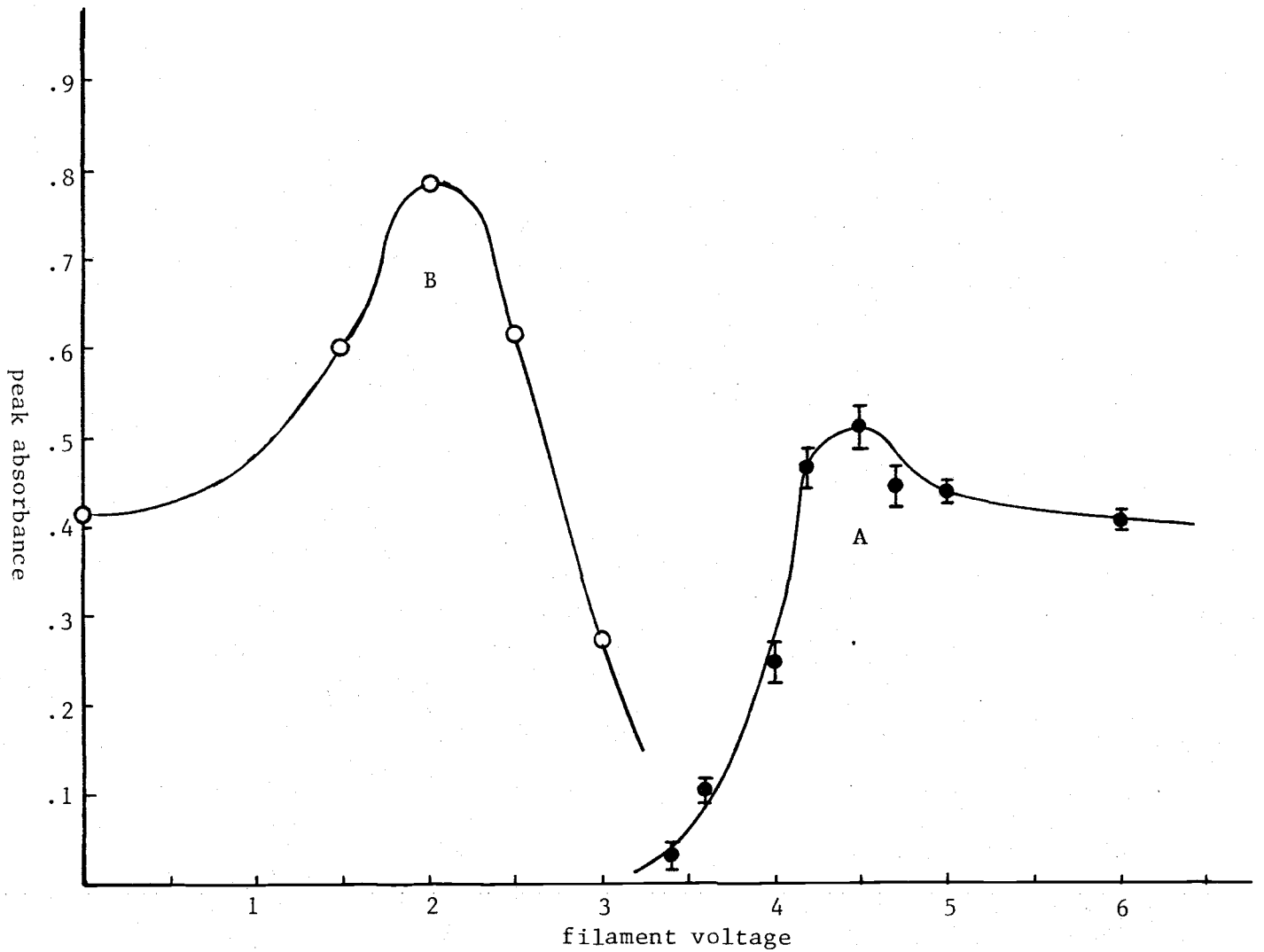

Figure 16. Filament prefire and fire voltage optimization study using .12 ng (2 µl of 0.06 ppm) Ca at 422.7 nm.

Prefire Voltage. The optimum prefire voltage was determined by the study summarized by curve B in Figure 16. Using a firing voltage of 6 V, a 0.12-ng Ca sample and a 2-l/min. argon flow rate, the prefire voltage was varied to determine its effect on the peak absorbance value. This graph indicates a drastic drop in peak absorbance when a voltage higher than 2.00 V was applied to the filament. This result was due to premature atomization which removed a fraction of the atoms before the actual absorption measurement. Therefore, a prefire voltage of 2.00 V which yielded a tungsten surface temperature of 1300 $\pm$ 30°C, measured in the same manner as the firing temperature, was chosen as the optimum value. Curve B in Figure 16, indicating how the prefire voltage affects peak absorbance, was obtained by going directly from the prefire step to the atomization step (6-V firing voltage) without allowing the filament to cool off. Peak absorbance values increased to a maximum at 2.00 V, at which time the premature atomization previously described became significant. These improved results might be due to the fact that the filament can reach maximum temperature faster when the filament is hot to begin with. When this graph is compared to the absorbance point at 6.00 V on curve A where the absorbance was measured without a "prefire" step, the advantage of this procedure becomes obvious.

4. Variables Influencing the Slope and Shape of the Analytical Curve

Prefire Cooling. Closely linked with these voltages and their effects on peak height are the prefiring procedures which affected the

shape of the analytical curve. This is illustrated in Figure 17 which shows two calibration curves for calcium of peak absorbance versus concentration for two prefire procedures. For the curve A the prefire was followed by a 20-second cooling off period before the sample was atomized. This curve shows a drastic bend towards the concentration axis. For curve B the prefire was followed immediately by atomization and shows little or no deviation from linearity. It was noted with the 20-second cooling off period that the percent transmittance peaks were about 25 percent wider at the half-height width using the Ca quantity indicated. From these results, the maximum fire temperature was reached more quickly, thus causing faster atomization and hence, narrower but taller peaks. Since peak broadening was less significant at higher quantities the calibration curves were more linear at higher analyte quantities.

Vertical and Horizontal Filament Position. Perhaps the most striking improvement in curve linearity was found in the comparison of the filament positioning; the horizontal versus the vertical filament. Figure 18 shows two Mg peak absorbance calibration curves for these two filament positions. The slopes of the curves are the same for both methods at low quantities of analyte (0-0.6 ng). However, at higher quantities the vertical filament sensitivity becomes drastically poorer. At the low levels where the two are comparable the detection limits as stated in Table II are similar with the horizontal filament yielding a value half as much as for the vertical position.

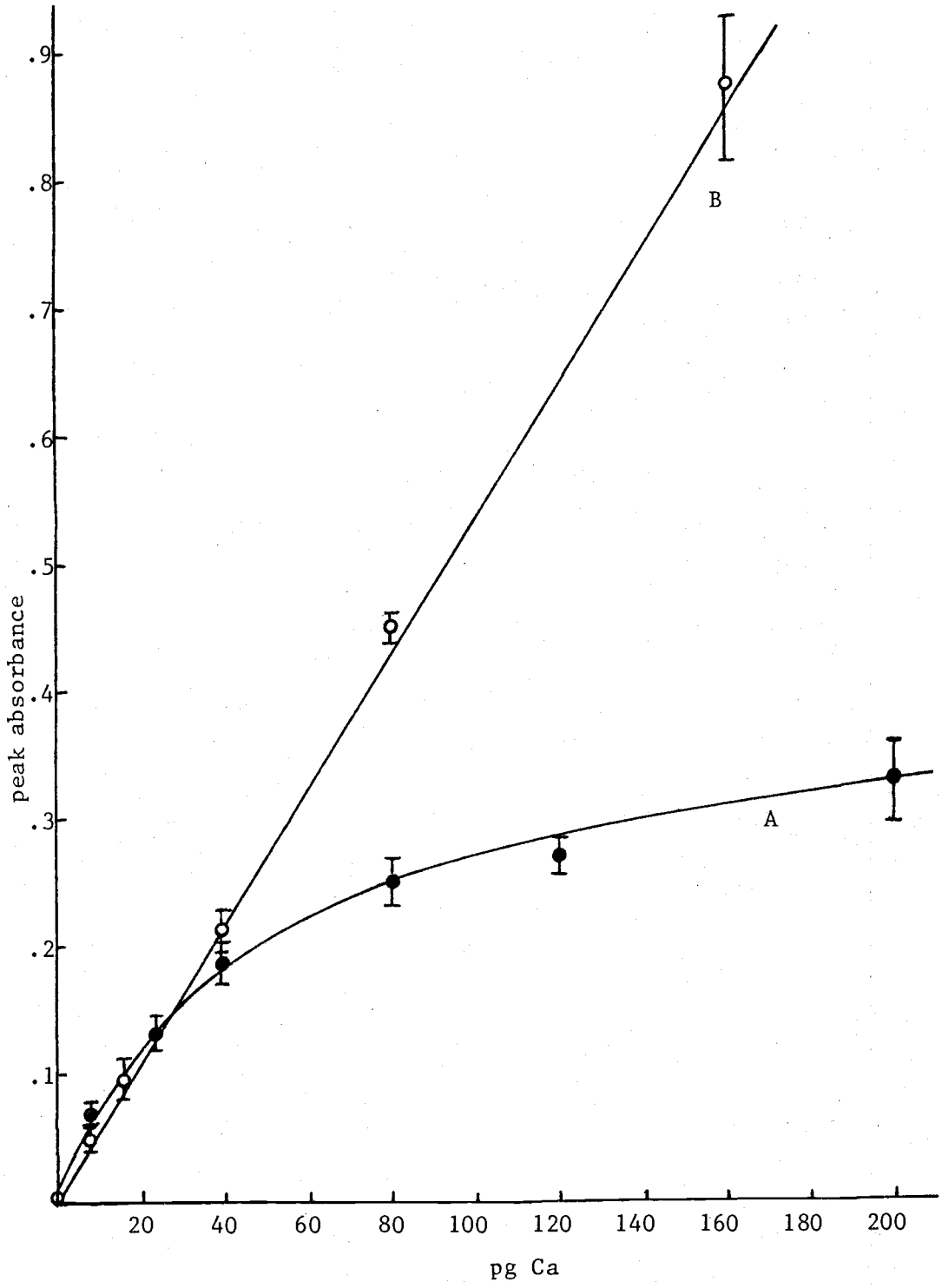

Figure 17. Calcium calibration curves with a 20-second cooling off period after prefire (solid points) and no cooling (open points) before atomization; wavelength = 422.7 nm.

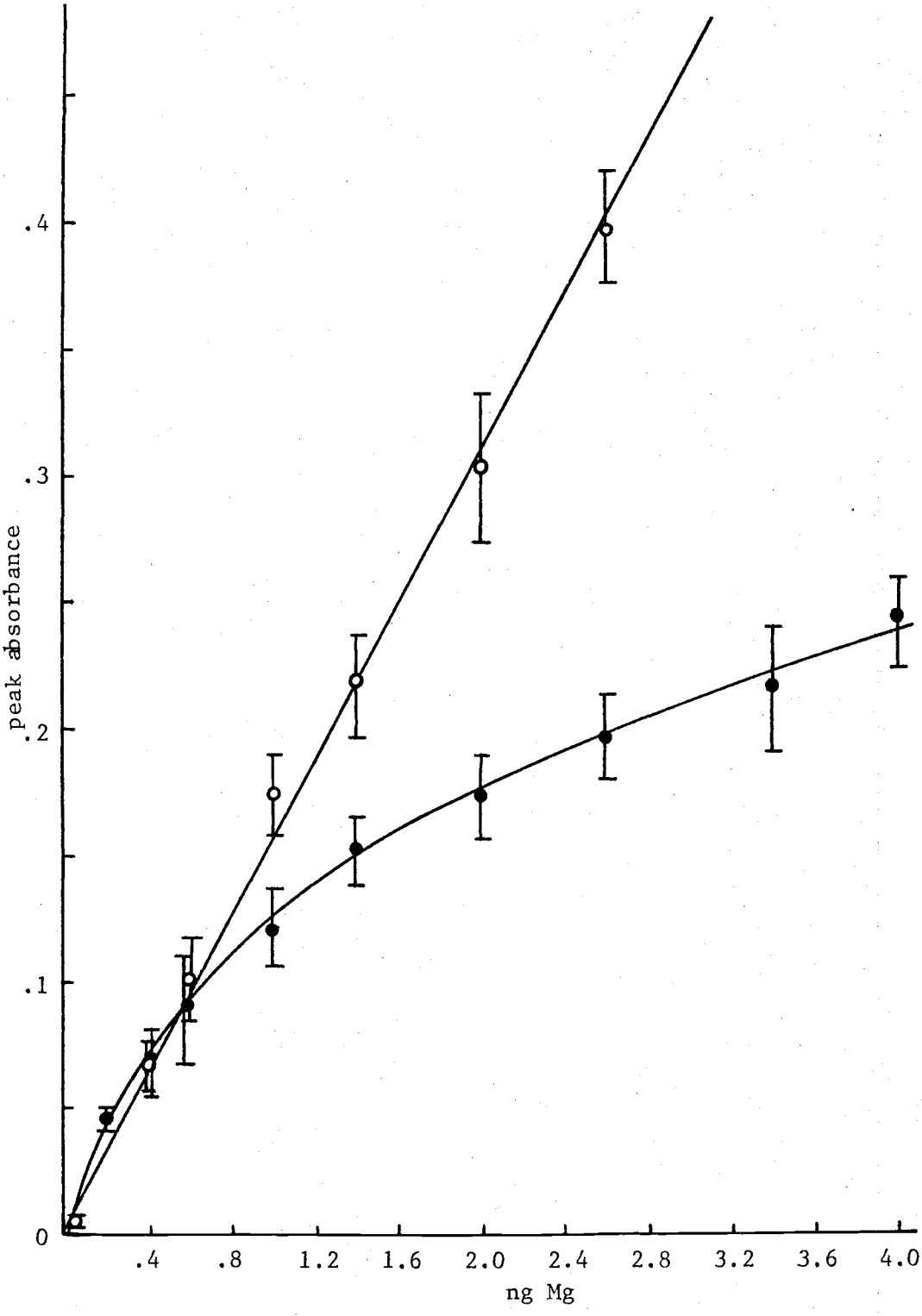

Figure 18. Magnesium calibration curve at 285.2 nm using vertical (solid points) and horizontal (open points) filaments using a firing voltage of 4 V and a sample size of 2 µl.

Since the earlier vertical filament study was performed at a 4-V firing voltage and a 7.5-l/min. argon flow rate, the horizontal position study was performed under the same conditions. The atoms produced were viewed by focussing the hollow cathode lamp 2 mm above the top of the vertical filament and at the optimum location inside the horizontal filament. In both cases, the "prefire" step was not included in the sampling procedure.

The slope of the peak absorption calibration curves are a complex combination of differing geometry, argon flow rate, temperatures at various points in the helix, absorption line profiles, atomization rate from the filament surface, effective optical path length, chemical recombination, etc. Therefore, it is difficult to theoretically predict exactly how the results for the two filament positions should differ from each other.

On the other hand, a brief discussion may help to provide a limited understanding of why the two filament positions give such different results. When atomization occurs for the vertical filament, the shape of the atomic vapor cloud can be considered cylindrical in nature, bounded roughly by the diameter of the helical filament and extending upward (due to the flow of carrier gas) into the viewing region located above the filament. Since atoms are deposited all along the filament during the drying step, they must travel different distances (1-4 mm) in order to reach the viewing region. These atoms absorb at different times resulting in broad absorption peak versus time profiles and lower peak absorbance values. However, when the

horizontal filament is used, all of the atoms are deposited on the filament essentially the same distance away from the optical axis, since the helix and the hollow cathode beam are concentric about the same axis. This results in a longer viewing path (the length of the helix compared to its diameter) where a higher percentage of atoms are viewed at one time. Therefore, the atoms enter the viewing region in a narrower time span resulting in narrower and more intense absorption peak versus time profiles. Although this argument may help to explain the increased peak absorbance sensitivity for the horizontal filament when high quantities of Mg are used, it does not explain why the sensitivities in Figure 18 are the same at low quantities.

Differences in the widths of the absorption line profile of the analyte atoms for the two filament positions might help to explain the equality. It seems likely that the atoms in the observation region above the vertical filament are in a cooler region than the atoms located in the hot core of the horizontal filament. The lower temperature reduces Doppler and collisional broadening of the absorption coefficient line profile (the two main sources of line broadening) and thereby increases the peak of the absorption coefficient line profile (absorptivity versus wavelength profile curve), since the integral of the absorption coefficient line profile must remain constant, a fundamental law. The absorption sensitivity is therefore greater for the cooler atoms in the observation region of the vertical filament than would otherwise be predicted by the argument in the previous paragraph. By a compensating coincidence the increased

sensitivity causes the two curves in Figure 18 to coincide within experimental error at low quantities. This mechanism also predicts a curvature at high quantities when the width of the emission line profile from the hollow cathode source is the same order of magnitude as the absorption coefficient line profile, as may be true for the vertical filament case. Curvature occurs because the wings of the emission source are not absorbed as much as the center of the line, causing the same affect as stray light.

B. Time-Integrated Absorbance

Absorbance peak integration proved to be the answer to most of the linearity problems inherent in peak absorbance calibration curves. Figure 19 compares the linear time integrated absorbance calibration curve with the nonlinear peak absorbance curve for copper. The problem of peak broadening which caused nonlinearity, especially at the higher analyte levels, was eliminated by using the absorbance area, and linearity was extended to regions where peak absorbances were greater than 1.0. Reproducibility and hence, detection limits (Table II) were improved since small changes in peak absorbance values due to atomization rate changes from one run to the next which caused peak broadening did not show up in the integrated results. Since the amplitude of the integration signal is proportional to the total area under the absorbance peak, more photons were observed and shot noise was reduced. This also helped to improve the signal-to-noise ratio and therefore, the detection limits. The only problems encountered

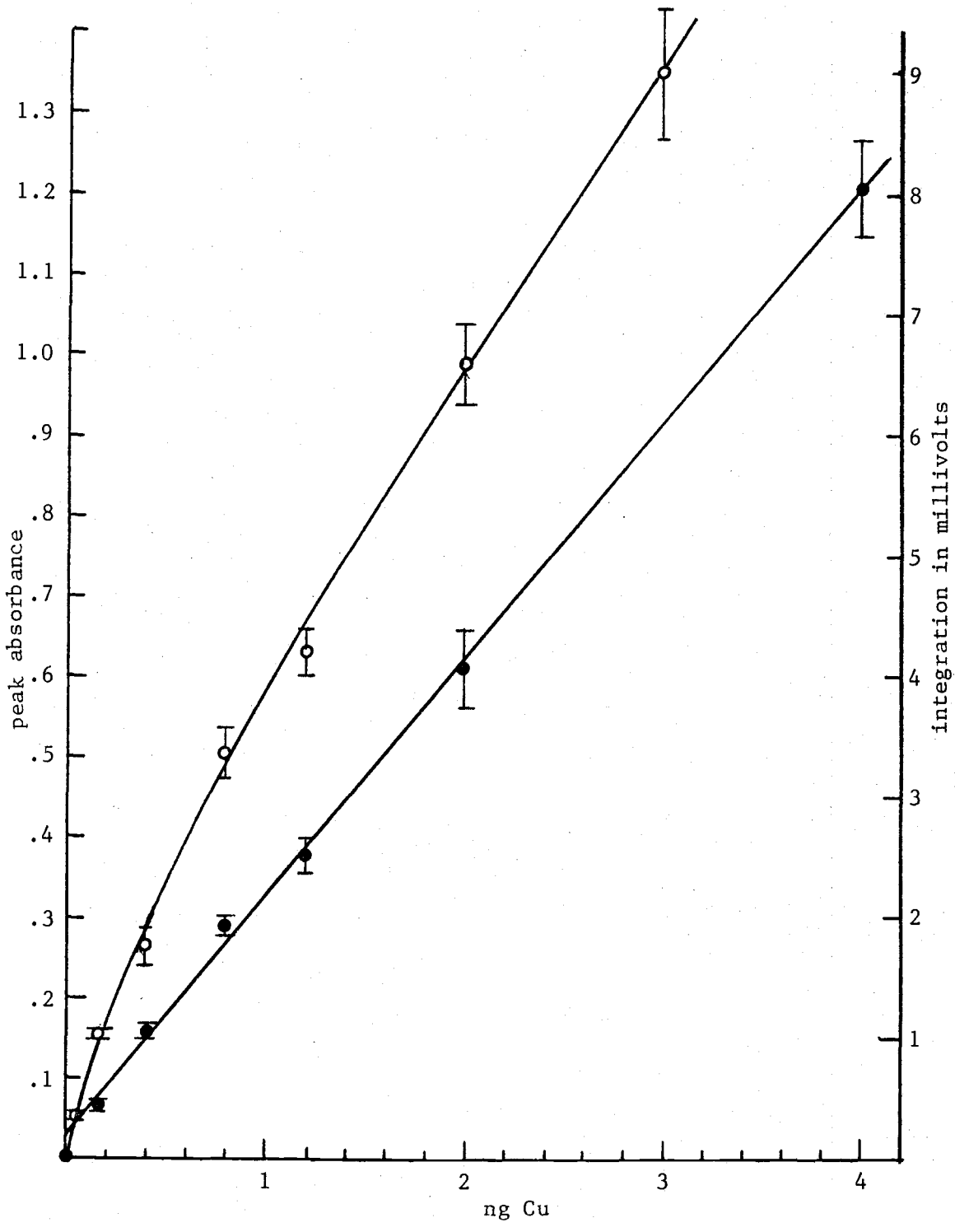

Figure 19. Copper calibration curves, absorbance (hollow points) and peak integration (solid points) versus concentration; wavelength = 324.7 nm.

using this technique were related to possible voltage drifts in amplifiers A_3-A_7 shown in Figure 5, inherent in the relatively inexpensive amplifiers available. Drifts were usually unidirectional fluctuations of 0.1-0.2 mV/sec., causing data recording problems, especially during low level measurements.

C. Summary of Analytical Results

Figures 11, 12, 17, 18 and 19 show the calibration curves for Ag, Ca, Mg and Cu illustrating the results of vertical and horizontal filaments and peak absorbance and integrated absorbance measuring techniques obtained with the instrumental settings stated in Table V. The sensitivities and limits of detection for these elements are given in Table II for the horizontal filament, juxtaposed with those of the other nonflame instruments summarized in the introduction.

The limit of detection for this study is defined as the concentration or quantity of the analyte which gives a signal equal to the signal-to-noise level (unity S/N) where the noise is defined as the peak absorbance standard deviation of replicate sampling. This definition was chosen in order that a direct comparison could be made between these results and those of Williams and Piepmeier (16) who used a vertical filament. A comparison of the results using the horizontal and vertical filament positions indicates that overall sensitivities were improved by factors of three to five and detection limits by factors of two to twenty by using the horizontal filament. Other authors in Table II did not state precise detection limit

definitions, so only an order of magnitude comparison can be made. However, when a rough comparison is made the horizontal filament is similar or better than these other instruments.

D. Phosphate Interference

A brief study of the interference of phosphate on calcium was conducted and is summarized in Figure 20. This graph shows the change in peak absorbance as the phosphate concentration is varied. The phosphate was found to suppress by about 20 percent the peak absorbance value observed without phosphate at higher phosphate concentrations. A similar influence has been found in other nonflame methods (20). It had no perceptible effect on the peak half-height width. That is, increased levels of phosphate did not cause broadening which could have explained the decreased peak absorbance value. Since the atomization temperature is at least several hundred degrees cooler than in most flames, it was expected that the interference effect would be greater for this atomizer, and indeed, this was the case. The shape of this curve is comparable to that of previous interference studies in flames; the curves tend to level off at a calcium to phosphorus mole ratio of two. This suggests that the influence is due to the formation of a calcium-phosphorus compound of low volatility as is known to be the case in flames.

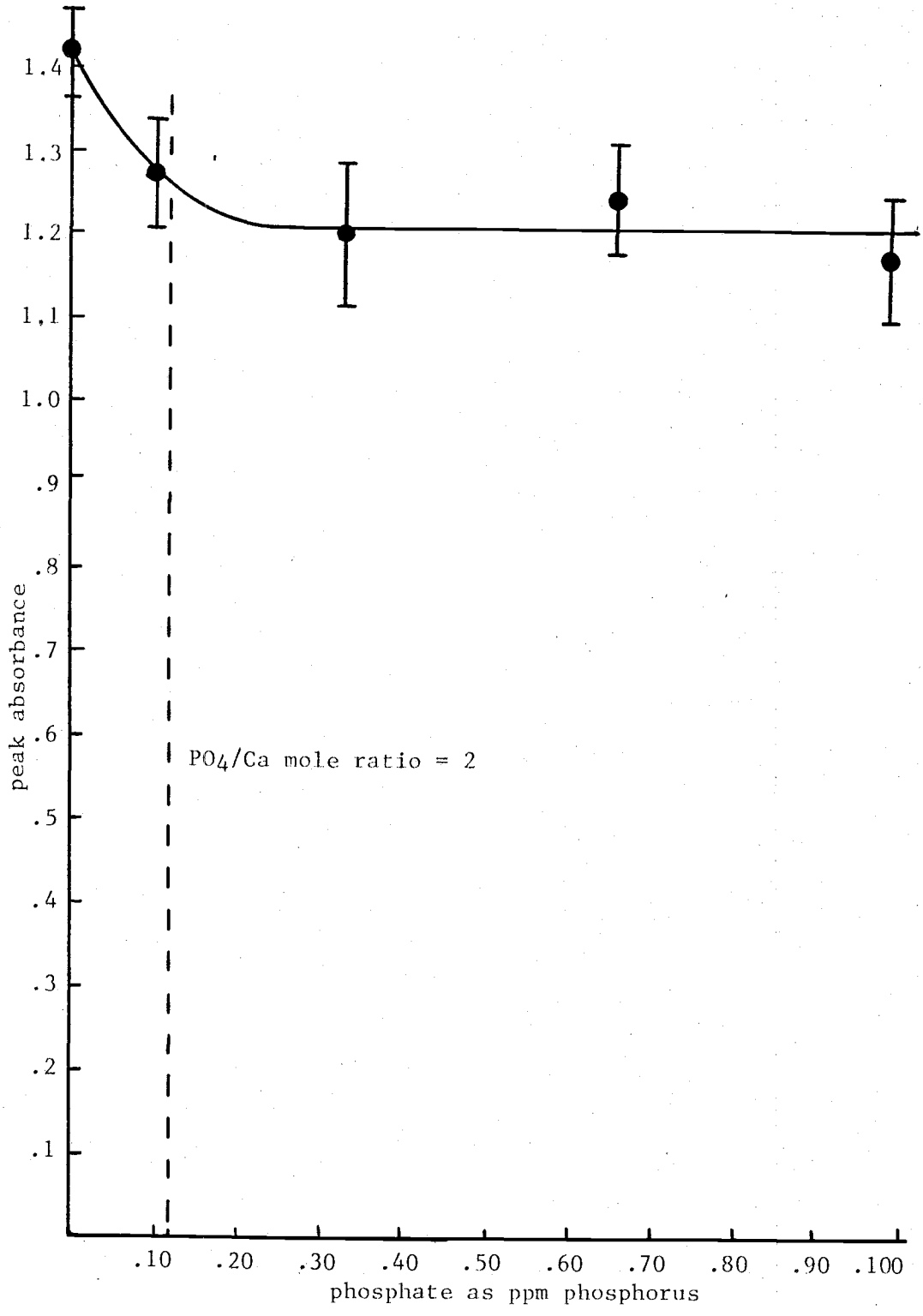

Figure 20. Phosphate interference on calcium; 2 µl of 0.08 ppm calcium is used.

V. CONCLUSION

The horizontal filament and the more sophisticated electronics have proven to be an improvement over the vertical filament of Williams and Piepmeier (16). Not only did the sensitivities and limits of detection generally improve, but peak absorbance values of up to 1.0-1.2 were readily achieved.

The improved filament mounting assembly, offering better protection for the helix, greatly increased the analytical lifetime of the filament. Filament replacement was also made easier and quicker.

The use of time-integrated absorbance in calibration curves solved the problems of linearity which peak absorbance measurements on the horizontal filament could only partially eliminate. In addition, since compensating changes in peak amplitude and peak broadening do not influence the integrated results, reproducibility and limits of detection are improved.

Integration may be important when analyzing non-ideal samples. Since the horizontal filament atomizes samples at a temperature 1000°C cooler than most carbon rods and furnaces, salt effects may tend to broaden peaks because of a lowering of the atomization rate. Theoretically the area under the peak will continue to be representative of the analyte as long as the salt matrix does not bind the analyte as in the phosphate interference on Ca.

The nonflame instrument has proven in certain cases to be a viable alternative to the more expensive carbon rod and furnace

atomizers. It is possible that it can be used with the type of flame spectrometers found in most analytical laboratories. Its power requirement is small enough so that an expensive precision high-current power source is not needed.

The tungsten filament method is inexpensive to operate. The bulbs themselves cost one dollar each and have lasted through 500-1,000 runs before replacement became necessary. Argon gas, the other expendable material, was used up at an almost unnoticeable rate, with one tank lasting for over six months of moderate to heavy use. Overall, it has proven to be easy to use and suitable for the routine analysis of numerous aqueous samples.

The matrix effects due to the low atomization temperatures are the greatest deterrent to this method. Salt interference and a possible pH dependence severely limit the use of this instrument. Only after laborious sample treatment could biological samples such as plant tissue or blood be analyzed. Work is needed to provide ways of eliminating or minimizing these problems. Such limitations restrict the use to ideal solutions or specially treated aqueous solutions such as metals dissolved in acid. However, this seems to be a common problem to all furnace techniques so far devised.

One aspect to investigate might be a different sample application method. For example, electroplating the metal in the sample onto the helix might result in fewer interferences. Such studies could lead to more versatile applications, more accurate and precise measurements, and therefore, wider use of such techniques as analytical tools.

VI. BIBLIOGRAPHY

1. Robinson, J.W. "Atomic Absorption Spectroscopy," New York, Marcel Dekker, Inc., 1966, p. 72.

2. Amos, M.D. "Nonflame atomization in AAS," American Lab 4(8):57. 1972.

3. L'vov, B.V. "The analytical use of atomic absorption spectroscopy," Spectrochim. Acta 17:761. 1961.

4. King, A.S. Astrophysical Journal 2(2):44. 1969.

5. L'vov, B.V. and G.G. Lebedev. Zh Prikl. Spektroskopie 7:264. 1967.

6. West, T.S. and Y.K. Williams. "Atomic absorption and fluorescence spectroscopy with a carbon filament atom reservoir," Analytical Chim. Acta 45:27. 1969.

7. Cantle, J.E. and T.S. West. "Ultramicro atomic-absorption spectroscopy with a tungsten filament atom-reservoir," Talanta 20: 459. 1973.

8. Robinson, J.W. and P.J. Slevin. "Recent advances in instrumentation in atomic absorption," American Lab 4(8):10. 1972.

9. Matousek, J.P. and B.J. Stevens. "A carbon rod atomizer for AAS," American Lab 3(6):45. 1971.

10. Massmann, H. "Vergleich von atomabsorption and atomfluoreszenz in der graphitkuvette," Spectrochim. Acta 23b:215. 1968.

11. Welz, B. and Z. Wiedeking. "Determination of trace elements in serum and urine using flameless atomization," Z. Anal. Chem 252:111. 1970.

12. Woodriff, R. and G. Ramelow. "Atomic absorption spectroscopy with a high-temperature furnace," Spectrochim. Acta 238:665. 1968.

13. Donega, H.M. and T.E. Burgess. "Atomic absorption analysis by flameless atomization in a controlled atomosphere," Analytical Chemistry 42:1521. 1970.

14. Bratzel, M.P., Jr., R.M. Dagnall and J.D. Winefordner. "A hot wire loop for atomic fluorescence spectrometry," App. Spect. 24(5):518. 1970.

15. Goode, S.R., A. Montaser and S.R. Crouch. "Optimization of instrumental parameters in an automated nonflame AF spectrometer," Applied Spect. 27(5):355. 1973.

16. Williams, M. and E.H. Piepmeier. "Commercial tungsten filament atomizer for analytical atomic spectrometry," Analytical Chemistry 44:1342. 1972.

17. McWilliam, I.G. and H.C. Bolton. "Instrumental peak distortion I. relaxation time effects," Analytical Chemistry 41:1755. 1969.

18. De Jong, G. and E.H. Piepmeier. "High intensity pulsed hollow cathode lamps," Unpublished thesis, Oregon State University, Corvallis, Oregon. 1973.

19. Price, W.J. "Analytical Atomic Absorption Spectroscopy," London, Heyden and Son, Ltd., 1974, p. 185.

20. Leyton, L. "Phosphate interference in the flame photometric determination of calcium," Analyst 79:497. 1954.